2024년 2월

박사학위 논문

Neuropeptides regulate embryonic salivary gland branching through FGFs/FGFRs signaling pathway

조선대학교 대학원

치의생명공학과

NGUYEN KHANH TOAN

Neuropeptides regulate embryonic salivary gland branching through FGFs/FGFRs signaling pathway

Neuropeptide는 FGF/FGFR 신호 전달 경로를 통해 배아 타액선형성 조절

2024년 2월 23일

조선대학교 대학원

치의생명공학과

NGUYEN KHANH TOAN

Neuropeptides regulate embryonic salivary gland branching through FGFs/FGFRs signaling pathway

지도교수 **안상건**

이 논문을 이학 박사학위신청 논문으로 제출함

2023년 10월

조선대학교 대학원

치의생명공학과

NGUYEN KHANH TOAN

NGUYEN KHANH TOAN의 박사학위 논문을 인준함

위원장 최 한 철 (인) 

위 원 유 재 식 (인) 

위 원 김 병 훈 (인) 

위 원 윤 정 훈 (인) 

위 원 안 상 건 (인) 

2024년 1월

조선대학교 대학원

TABLE OF CONTENTS

LIST OF FIGURES

LIST OF TABLES

국문초록

Neuropeptide는 FGF/FGFR 신호 전달 경로를 통해 배아 타액선형성 조절

NGUYEN KHANH TOAN
지도교수 안상건
치의 학과
조선대학교 대학원

타액선 분지형성은 신경 신호전달의 기능적 통합에 의해 조절되지만, 기본적인 기전은 명확히 규명되지 않았다. 본 논문에서 우리는 신경전달물질인 SP와 NPY가 노화 마우스 Kl-/- 의 배아 타액선에서 분지형태형성에 영향을 주는지 조사하였다. Kl-/- 마우스 배아 타액선의 형태학적 분석 및 면역염색 분석에서 상피아 형성, 신경 세포 증식/분화, 유관 세포의 타액선 기능적 마커인 ZO-1의 감소를 확인하였다. SP/NPY의 48h 처리는 분지형태형성, 부교감신경분포와 상피세포의 증식을 유도하였다. ERK 억제제 U0126은 배아 타액선에서 신경 물질에 의해 유발된 상피아 형성을 특이적으로 억제하였다. RNA-seq profiling 분석은 배아 타액선(E15)에 SP/NPY 처리가 FGFs/FGFRs의 발현을 유의성있게 조절한 것을 밝혔다. FGFR억제제인 BGJ389는 SP/NPY 처리와 ERK1/2 발현에 의해 유도된 신생 분지형성을 억제한다. 이러한 결과는 신경 펩티드 인 SP/NPY가 FGFR/ERK1/2 매개된 신호전달을 따라 배아 타액선의 발달을 유도하는 것을 보여준다.

ABSTRACT

Neuropeptides regulate embryonic salivary gland branching through FGFs/FGFRs signaling pathway

Nguyen Khanh Toan
Advisor: Prof. Sang-Gun Ahn, Ph.D.
Department of Pathology, School of Dentistry,
Graduate School of Chosun University

Salivary gland branching morphogenesis is regulated by the functional integration of neuronal signaling, but the underlying mechanisms are not fully understood. Here, we investigated whether the neuropeptides SP and NPY affect the branching morphogenesis of embryonic salivary glands in aging $Kl^{-/-}$ mice. In the salivary glands of embryonic $Kl^{-/-}$ mice, morphological analysis and immunostaining revealed that epithelial bud formation, neuronal cell proliferation/differentiation, and the expression of the salivary gland functional marker ZO-1 were decreased in ductal cells. Incubation with SP/NPY for 48 h promoted branching morphogenesis, parasympathetic innervation and epithelial proliferation. The ERK inhibitor U0126 specifically inhibited neuronal substance-induced epithelial bud formation in the embryonic salivary gland. RNA-seq profiling analysis revealed that the expression of FGFs/FGFRs was significantly regulated by SP/NPY treatment in the embryonic salivary gland (E15). The FGFR inhibitor BGJ389 inhibited new branching formation induced by SP and NPY treatment and ERK1/2 expression. These results showed that the neuropeptides SP/NPY induced embryonic salivary gland development through FGFR/ERK1/2-mediated signaling.

I. INTRODUCTION

Salivary glands are essential component in human daily activity, playing crucial roles in food digestion and maintaining oral health [1]. The main roles of these glands are producing and secreting saliva, a fluid that participated in multiple roles, includes initiate food digestion, maintenance of oral pH, protection of oral structures, and assistance in speaking and articulation through lubrication [1,2]. Saliva loss, also known as hyposalivation, can lead to painful and devastating oral condition and deterioration of oral health, including difficulty in eating, increased dental decay, disrupted oral homeostasis, increase oral disease and periodontitis [3]. Hyposalivation is commonly observed in head-and-neck cancer patients, often as a consequence of radiotherapy treatment. It can also manifest as a result of autoimmune diseases such as Sjögren's syndrome, adverse effects of medications, or the natural aging process [3-5]. In contrast to younger individuals, salivary glands from aged population exhibits acinar atrophy, ductal dilation, reduced blood vessel density, and increased deposition of fibro-adipose tissue. Additionally, there's an upsurge in immune response signals, heightened infiltration of inflammatory cytokines, accompanied by a decrease in mitochondrial numbers and impaired oxidative phosphorylation [4,5]. All these age-associated alterations in salivary gland morphology and function contribute to the physiological changes observed in the elderly [4]. Despite substantial research on xerostomia and dry mouth syndrome treatments, success has been limited, as evidenced by numerous clinical trials yielding minimal outcomes and no permanent solution to restore damaged acinar cells in the salivary gland [3].

Klotho-deficient ($Kl^{-/-}$) mice model is an accelerated aging mice model that also developed postnatal salivary gland dysfunction [6]. $Kl^{-/-}$ mice displayed hyposalivation, smaller glands, less connective tissue, and fewer granular ducts and serous acini than WT littermates. [7,8]. Downregulation of growth factors, transcription factors and ion pumps are observed in the Klotho-deficient mice salivary gland [8,9]. Subsequent studies also demonstrated that multiple metabolic pathways in the salivary glands of Klotho-/- mice are dysfunctional,

including acetylbiosynthesis, ascorbic acid biosynthesis, and glutathione pathway in salivary glands [10,11]. Neuropeptides are small proteins that secreted by neurons, which mostly bind to G-protein coupled receptors to stimulate long term effect in the nervous system, and thus, impact majority the innervated organs [12]. Impacts of neuropeptides in salivary glands varied from basic functions such as stimulating protein and fluid secretion. to complicated ones such as modulating immune response, facilating salivary gland development, or being involved in feeding behavior. [13-16].n the other hands, several neuropeptides can induce hyposalivation, such as opioids [17]. NPY and SP are two neuropeptides that are capable of induce protein and fluid secretion in salivary gland, and possess great potential in regenerative medicine [18,19]. NPY and SP were successfully applied in cardiovascular regeneration, wound healing, neurogenesis, and anti-aging [20-23]. We designed this study, using *ex vivo* embryonic salivary gland culture system, to investigate the embryonic salivary gland development in the aging-accelerated $Kl^{-/-}$ mice and evaluate the potential impact of neuropeptides NPY and SP toward salivary gland.

In this study, we demonstrated that the embryonic salivary gland of $Kl^{-/-}$ mice, while resembling similar morphology and development process, exhibits lower number of epithelial buds, as well as had lower expression in neuronal and ductal markers. Treatment of neuropeptide NPY and SP can promote the branching morphogenesis, neurogenesis and epithelial proliferation of salivary gland in both $Kl^{-/-}$ and $Kl^{+/+}$ mice. Beneficial effect of neuropeptide NPY and SP are dependent on the FGF/FGFR/ERK signaling, as demonstrated through loss-of-function experiments. Our data provided a novel insight in the potential function of neuropeptide NPY/SP in the development of embryonic salivary gland.

II. BACKGROUND

2.1. Salivary glands

Salivary glands are essential component in human daily activity, playing crucial roles in food digestion and maintaining oral health [1]. The main roles of these glands are producing and secreting saliva, a fluid that participated in multiple roles, includes initiate food digestion, maintenance of oral pH, protection of oral structures, and assistance in speaking and articulation through lubrication [2]. 90 percent of saliva are secreted by three major glands; the parotid, submandibular and sublingual glands, while numerous minor glands produced the remaining 10% [24]. Saliva, the primary secretion of the salivary glands, is composed of water, electrolytes, mucins, enzymes, growth factors, and antibacterial substances [4,25-28]. The production of saliva is regulated by the autonomic nervous system, specifically the parasympathetic division, which stimulates salivary gland activity in response to sensory stimuli such as the smell, sight, or taste of food [29]. The main secretory component in the salivary gland are acinar cells, which are bundled together by lateral membranes and tight junction proteins, called acini [1]. Acini and its secretion product are depending on the composition of acinar cells, either serous, mucous or seromucous [30]. Secreted saliva from acini will be modified and transported through the ductal system [31]. Other components that created the salivary glands microenvironments are myoepithelial cells, extracellular matrix, sympathetic and parasympathetic nerves, a diverse population of immune cells, an intricate microvasculature system, as well as adipose and muscle tissue [32-35].

2.2. Saliva

Saliva, the primary secretion of the salivary glands, is composed of water, electrolytes, mucus, enzymes, and antibacterial substances. Despite participating in multiple essential roles, the importance of saliva only noticed when it is absent. Saliva loss, also known as hyposalivation, can lead to painful and

devastating oral condition and deterioration of oral health, including difficulty in eating, increased dental decay, disrupted oral homeostasis, increase oral disease and periodontitis [3]. Hyposalivation usually occurred in head-and-neck cancer patients, as a side effect of radiotherapy treatment; or as a result of autoimmune disease like Sjögren's syndrome; or even from the side effects of medication or from the natural aging process [1,3,4].

Saliva secretion is a two stages process that is controlled by calcium level [31, 36]. Dysregulation of calcium signaling associated with salivary gland dysfunction [36]. In the first stage, calcium (Ca^{2+}) is released from endoplasmic reticulum, raising intracellular Ca^{2+} concentration; which activates multiple ion channels and recruits the water-secretion channel Aquaponrin5 (Aqp5) to the apical acinar membranes [37]. As a result, an isotonic, sodium (Na^{+}) and chloride (Cl^{-}) ion rich fluid is released into the lumen of acini [31]. In the second stage, as the initial fluid travels through the ductal system, epithelial sodium channel (ENaC) and the cystic fibrosis transmembrane conductance regulator (CFTR) induces the Na^{+} and Cl^{-} reuptake into ductal cells [38]. Bicarbonate (HCO_3^{-}) is released to saliva through both CFTR and solute carrier family 26 member 6 (Slc26a6), resulting in a hypotonic, neutral pH saliva [38-40].

Saliva secretion is initiated after receiving signal from nervous system. It is wildly accepted that the water and electrolyte release from acinar cell is regulated by parasympathetic nervous system, while protein and mucin secretion is controlled by sympathetic nerves signaling [29,31,32]. Acetylcholine, the main neurotransmitter in the parasympathetic nervous system, activates G protein-coupled receptors muscarinic receptors M1 and M3 to induced the production of inositol triphosphate (IP3). IP3 binds to IP3 receptors in the endoplasmic reticulum leading to release of Ca^{2+} from internal storages, raising intracellular Ca^{2+} concentration [41-43].

Sympathetic nervous system controls saliva secretion through α and β-adrenergic receptors. Since these receptors are also coupled with different

G-proteins, activation of these receptors by epinephrine and norepinephrine also resulted in elevation of intracellular Ca^{2+} level [44]. Additionally, selective activation of α1 adrenergic receptors by phenylephrine induces Aqp5 translocation to membrane through cyclic guanosine monophosphate (cGMP) and protein kinases G (PKG) signaling pathway [37]. Furthermore, activation of β adrenergic receptors also raising intracellular Ca2+ concentration through cyclic adenosine monophosphate (cAMP) and protein kinases A (pKA) pathway [45,46]. Finally, several nonadrenergic, noncholinergic neuropeptides can stimulate saliva secretion, such as substance P (SP) and vasoactive intestinal peptide (VIP). VIP stimulates protein secretion through cAMP/PKA pathway, while SP binds to neurokinin 1 receptors and induce production of IP3 to increase intracellular Ca^{2+} concentration [47].

2.3. Salivary gland development

In mammalian; salivary gland contains three major component - submandibular gland (SMG); sublingual gland (SLG) and parotid gland (PG), and several minor glands. Salivary gland development started at embryonic day 11 (E11) in mice; at gestational age week 6 in human and continue postnatally [29-32]. The developmental pattern is consistent in both human and mice: Epithelial cells multiplied and thickened the oral epithelium layer, which invaginated into a loosen mesenchyme to form the initial bud. Mesenchyme then condensed while the epithelial cells from the epithelial buds started to extends deeply and branched extensively into the underlying mesenchyme and differentiated into acinar and ductal cells; which is called branching morphogenesis [48-51].

Embryonic salivary gland development was studied exhaustively using the organic culture of murine embryonic SMG as model. In detail; there are five stages in the embryonic salivary gland development: (1) Prebud stage, (2) Initial bud stage, (3) Pseudoglandular stage, (4) Canalicular stage and (5) Terminal differentiation stage.

Prebud stage (E11.5 - 12.5 in murine embryos): Proliferation of oral

epithelium was induced by mesenchymal-epithelial interaction. The sign of this stage is the formation of an epithelial placode from the thickened oral epithelium, also called the prebud [30].

Initial bud stage (E12.5 – 13.5 in murine embryos): The epithelial placode invaginated into the condensing mesenchyme, formed a plant-like structure with a spherical epithelial bud and a long epithelial stalk, which eventually developed into the main duct [51]. The neuronal-epithelial interaction started in this stage, with the neuronal precursor wrapped around the epithelial stalk and coalesce to form the submandibular parasympathetic ganglia [52,53]. The basement membrane divided the epithelial bud from the mesenchyme, stabilized the epithelium structurally and actively participated in the branching morphogenesis in later development stage [49]. During this stage, the mesenchyme continued its condensation, which eventually formed the capsule of salivary gland [49].

Pseudoglandular stage (E13.5 – E14.5 in murine embryos): This staged is marked by extensive branching of the epithelium through multiple successive rounds of cleft formation, duct elongation, and duct lumen formation. Epithelium buds extended to the condensed mesenchyme, created new stalks from the main duct [49]. At the same time, clefts formed on the peripheral area of the epithelial buds, separated the epithelial cells at the location, then deepened and divided the primary buds into daughter ones [54]. In the epithelial stalks, ductal lineage cells differentiated into basal cell layer and luminal cell layer, and the keratin 19 (Krt19) – expressing luminal cells started to condense at the midline of the stalks [14]. Microlumens are generated from the apical membrane of these polarized Krt19+ luminal cells; then microlumens merged to create a continuous lumen across the midline of the stalks [14].

Canalicular stage (E14.5 – E15.5): This staged is marked by the expanding of lumen in the stalks, creating the “canal” or tube for fluid secretion in the future. Luminal cells at the center of lumen went through apoptosis while

these one around the new formed lumen proliferated. Initially, these observed differential apoptosis was considered as the main mechanism driving the lumen expansion to create a hollowed tube, however, it was revealed that neuropeptide vasoactive intestinal peptide (VIP) regulated the lumen expansion/tubulogenesis through increased flow of electrolytes and fluid transport [14,49].

Terminal differentiation stage (E15.5 forward): This stage began when the ducts and acini are completely hollowed out and continued postnatally. Epithelial cells both differentiated morphologically and functionally during this stage. Ductal cells developed into excretory, striated, and intercalated ducts while acinar cells developed into serous or seromucous secretory acini, as well as myoepithelial cells.

Development of embryonic salivary gland are orchestrated by multiple signaling pathways that regulated the interaction between epithelium and mesenchyme, which was reviewed thoroughly in previous literatures [48-56]. Among these developmental pathways, fibroblast growth factors (FGF) signaling and epidermal growth factors signaling (EGF) are two major drivers of salivary gland organogenesis.

FGF system involves 23 secreted FGFs and 4 transmembrane tyrosine kinase receptors and its involvement in salivary gland development was well-recorded. Fgfr2b or its ligand Fgf10 knockout model failed to develop its salivary glands as well as other epithelial organs, including lungs, kidneys, and pancreas [58,59]. Even delete one allele of either Fgfr2b or Fgf10 leading to hyposalivation due to hypo-plasticity of submandibular salivary gland [60, 61]. Recently, it was discovered that Fgfr1 and Fgfr2 signaling exhibits combinatorial function in regulation of salivary gland development [62]. Although inactivation of single allele of Fgfr1 doesn't reduce branching; fully knockout of Fgfr1 reduced branching morphogenesis significantly in the presence of intact Fgfr2. Alternatively, losing one allele of Fgfr2 significantly reduced branching to the similar level of Fgfr1 knockout model, and knockout

of Fgfr2 severely hampered the salivary gland organogenesis [62]. *In vitro* supplementation of FGF1, FGF2, FGF7, and FGF10 induced branching morphogenesis of epithelial structures [63]. However, deletion of negative regulator of FGF signaling Sprouty (Spry) leading to excessive FGFs signal, which in turn prevents parasympathetic innervation, gangliogenesis and reduced progenitor cell population significantly in embryonic salivary glands [52].

The mechanism of how FGF signaling in salivary gland development are well-defined through exhaustive researches [1, 48]. Activation of FGF signaling activates its canonical downstream pathway, particularly MAPK/ERK1/2 and PI3K pathways, which is involved in proliferation of epithelial cells and expansion of epithelial buds [63]. Fgfr2b activation induced Kit signaling and expanded the KIT+K14+SOX10+ epithelial progenitor cells in the end buds, which is essential for new branches formation [64]. A recent study revealed a non-canonical pathway of Fgfr1/Fgfr2 system that regulate branching morphogenesis through modulation of basement membrane and cell-cell adhesion [62].

The EGF system plays a crucial role during organ development, morphogenesis, repair, and epithelial regeneration [65]. EGF ligands can bind to four kinase receptors, EGFR/Erbb1, Erbb2, Erbb3, and Erbb4 [1, 48]. The EGFR-null SMG has smaller SMG, reduced cell proliferation, and branching morphogenesis [66]. Similarity, Erbb3 knockout mice exhibits smaller SMG due to impaired acinar specification, while remaining an intact ductal system [67]. EGF, a ligand for Erbb1, mediates end buds branching through ERK-1/2 and PI3K pathways, while inhibition of PKC signaling greatly boosted EGF-induced branching [68]. Additionally, Acetylcholine signaling induced epithelial morphogenesis and maintained proliferation of keratin 5-positve progenitor cell in an EGF-dependent manner [53]. Acinar specification is driven through a neuronal-epithelial interaction between (NRG1)-ERBB3-mTORC2 signaling [67].

2.4. Aging and salivary gland dysfunction

Up to date, multiple histological alteration and functional reduction were observed in the salivary glands of elder population, however, there were no clear explanation about the cellular and molecular mechanisms that leading to the aging-induced salivary gland dysfunction [4,5]. Histological analysis from human, naturally and accelerated aging mice model illustrated that aging salivary gland exhibits acini atrophy, ductal dilation, lower vessel density and increased in fibro-adipose tissue deposition [4,5]. Additionally, there is an increase in the immune response signal, increased infiltration of inflammatory cytokines, paired with reduction in mitochondrial number and impaired mitochondrial function [5]. In the aged salivary gland tissues, a decline in both proliferation activity and number of stem cells were observed, therefore the endogenous regeneration of acinar in salivary gland could be slowed down [69]. Systemic meta-analysis summarized evidences that aging induced a medication-independent loss of unstimulated saliva in human [70]. Aging-induced structural deterioration in salivary gland secretory components lead to a reduction in saliva mucin protein and antioxidants [5,71]. Salivary dysfunction usually leads to hyposalivation and xerostomia, leaving a great burden in quality of life, especially after the COVID-19 pandemic [1,3]. Unfortunately, most of the approved medications for hyposalivation and xerostomia are artificial saliva and secretagogues, which came up with several shortcomings. Commercially available artificial saliva mimics the viscosity of saliva, but failed at all other aspects, including elasticity, lubricity and antibacterial [3,72]. Notably, commercial artificial saliva failed to prevent bacterial adherence, an important role of saliva in protecting oral structures [72]. Medication that are capable of stimulating saliva secretion are parasympathomimetic drugs that target muscarinic receptors M1 and M3 [3]. However, due to the widespread of non-neuronal cholinergic system, these medications usually associated with undesired, severe side effects, including vomiting, vasodilation, hypotension and bradycardia [3]. Other intervened

methods, such as transplantation of stem cells or bioengineered organoid, and viral-based gene therapies, are still in clinical trials [1,3]. Therefore, it is an urgent need to develop novel and sustainable therapy for salivary glands dysfunction, to improve living quality of elder population and patients suffered from hyposalivation and xerostomia.

2.5. Klotho

Klotho is an anti-aging protein discovered on 1997 by Dr. Kuro-O. Klotho deficient mice are indistinguishable compare to wild type and heterogenous littermate, but exhibits multiple aging-resemble phenotypes after 4 weeks old, including growth retardation, hyperphosphatemia, hypercalcemia, osteopenia, pulmonary emphysema, cognitive impairment, and multi-organ atrophy [6]. Klotho expression inversely correlated with aging and aging-related diseases progression, including Alzheimer's disease, kidney injury, vascular disease, muscular dystrophy and diabetes. Overexpression of klotho increased life span in rodents by approximately 20-30%, as well as therapeutic effects against multiple disease, such as mitigating amyloid-β accumulation in Alzheimer's disease, delaying the progression of chronic kidney diseases, and inhibiting tumor progression and drug resistance [73-77].

The most well documented function of Klotho is its involvement in the homeostasis of phosphate, calcium and vitamin D; which is maintained by the triangles of intestinal absorption, renal secretion/resorption and mobilization/storage in bones [78]. Klotho is an essential co-factor for fibroblast growth factor 23 (FGF23) and plays a crucial role in enhancing the interaction between FGF23 and fibroblast growth factor receptors (FGFRs) [79]. Klotho can bind to either FGF23 or FGFRs, which increases the affinity of FGFRs to FGF23 and stabilize the ligand/receptors interaction, thereby initiating downstream signaling cascades of FGF23 signaling pathways [79].

The relationship between klotho and FGF23 was discovered from the similarity of phenotypes between klotho-deficient mice and FGF23-deficient mice, including growth retardation, premature death and hyperphosphatemia [79].

FGF23 is a hormone that mainly produced in the bone cells that target kidney cells at the proximal renal tubule. Both Klotho and/or FGF23 could suppress expression of sodium-phosphate cotransporters (NaPi-2a and NaPi-2c), thus reduces renal reabsorption of inorganic phosphate (P_i) from urine [80,81]. In a klotho-dependent manner, FGF23 inhibits the expression of 25-hydroxyvitamin D 1-α-hydroxylase and induces the expression of 1,25-dihydroxyvitamin D 24-hydroxylase, two enzymes that catalyzes the synthesis and degradation of calcitriol, the physiologically active form of Vitamin D [82].

FGF23-mediated regulation of vitamin D biosynthesis is critical in maintaining calcium and phosphate homeostasis. By preventing excessive production of calcitriol, FGF23 helps to reduce the absorption of dietary calcium and phosphate, instead promoting their excretion [82]. Besides the effect of Klotho/FGF23 signaling, Klotho also regulate mineral homeostasis through transient receptor potential cation channel subfamily V (TRPV channels). Klotho possesses the enzymatic activity of β-glucuronidase, which allow it to hydrolyze the extracellular sugar residues of TRPV2/5/6 channels, stabilizing the channel in the cellular membrane and stimulating its activation, thus promote Ca^{2+} reabsorption into the renal and pancreatic β cells [83, 84].

Another important function of klotho is its participation in modulation of reactive oxygen species (ROS), which is mainly produced in mitochondrial during cellular respiration. Supplementation of exogenous klotho effectively reduces oxidative stress and mitochondrial damage [85-87]. Klotho can promote expression of several antioxidants, including manganese superoxide dismutase (Mn-SOD) and heme oxygenase-1 (Ho-1), through activating both Keap1-Nrf2 and FoxO transcription factors [88,89]. Additionally, recent studies suggested that Klotho can ameliorate mitochondrial dysfunction through inhibition of Wnt/β-catenin pathway and promote autophagy clearance through activation of AMPK/PGC1α pathway, which induce nuclear translocation of transcription factor EB (TFEB) [90].

2.6. Salivary gland dysfunction in Klotho deficient ($Kl^{-/-}$) mice

Dwarfism, organ shrinkage, organ deterioration, and a shorter life span were all observed in Klotho-deficient mice [6]. The initial study on the klotho finding indicated that klotho deficiency caused harm to a wide range of organs, including the stomach, thymus gland, gonads, lungs, skin, bones, and muscles [6]. Further research indicated that the salivary glands are also affected. Klotho-deficient mice had hyposalivation, reduced gland diameters, lack of connective tissue, and fewer granular ducts and serous acini than WT littermates [7,8]. Downregulation of epidermal growth factor (EGF), nerve growth factor (NGF), connective tissue growth factor (CTGF) and intracellular ion pump such as sodium/potassium-transporting ATPase subunit alpha-2 (ATP1a2) and sarcoplasmic/endoplasmic reticulum calcium ATPase 1 (ATP2a1) in the Klotho-deficient mice salivary gland [7,8]. Subsequent studies demonstrated that multiple metabolic pathways in the salivary glands of Klotho-/- mice are dysfunctional, including acetylcholine biosynthesis, the ascorbic acid biosynthesis pathway, and the glutathione pathway in salivary glands [10,11]. In particular, the levels of antioxidant glutathione as well as several precursors in glutathione biosynthesis, including cysteinyl-glycine, cysteine, and glutamyl-cysteine, are depleted in the salivary glands of klotho-deficient mice [10]. A similar pattern was observed in ascorbic acid biosynthesis, with a reduction of precursor glucose-6-phosphates, UDP-glucuronic acid, D-glucuronic acid, and L-ascorbic acid [11]. Finally, in the acetylcholine biosynthesis pathway, the expression and concentration of the catalytic enzyme choline acetyltransferase (ChAT) were depleted in klotho-deficient mice [10]. These findings revealed that the loss of klotho had a multi-factorial influence on the salivary gland from a histological, genetic, metabolic, and functional perspective.

2.7. Neuropeptide and salivary gland function

Neuropeptides are small proteins that secreted by neurons, which mostly bind to the G-protein coupled receptors to stimulate long term effect in the nervous system, and thus, impact majority the innervated organs [12]. More than 60 families of neuropeptides were discovered across 500 different species [91]. This sheer number makes neuropeptide one of the biggest and most diverse group of molecules that facilitate intercellular communication and play critical role in multiple biological processes, ranging from the macro level (behavior modulation, physiological regulation) to micro level (alternation of signaling pathway) [91].

The biosynthesis of neuropeptide started with the translation of encoded DNA into inactive precursors, pro-neuropeptides that requires protease activity to generate active neuropeptides (usually range from 3-40 amino acids) [12]. Several proteases have been identified to participate in neuropeptide biosynthesis pathway, including cysteine proteases cathepsin L, cathepsin H, cathepsin V and serine proteases proprotein convertase 1/2/3. The active neuropeptides are usually flanked by dibasic (Lys-Lys; Lys-Arg; Arg-Arg and Arg-Lys), and monobasic Arg residues [92]. Multiple neuropeptides can be generated from a single pro-neuropeptide, such as opiod hormones proenkephalin (PENK) and Prodynorphin (PDYN) [91,92].

The summary of neuropeptide family effect on salivary glands are listed on Table 1. Beside basic function like stimulating/inhibiting protein and fluid secretion, several neuropeptides exhibits more complicated impact in modulation of immune response, facilitated salivary gland developments, or involved in the feeding behavior (as saliva's role is aiding for food digestion and tasting). Several neuropeptides are used as potential biomarkers for quick and non-invasive testing using saliva as primary sources [93,94].

Table 1: Impact of neuropeptides on salivary glands function

Neuropeptide family	**Impact toward salivary glands**	**References**
ACBP/DBI	Inhibits saliva secretion	[95]
Adrenomedullin	Antibacterial, promote epithelial proliferation	[96,97]
Bombesin	Maintains salivary gland immunity	[98]
Bradykinin	Modulate pro-inflammatory cytokine expression, stimulate cytosolic Ca^{2+} signaling	[15]
Calcitonin and Calcitonin-related peptides	Facilitate Ca^{2+} signaling in submandibular ganglion; capable to stimulate peroxidase secretion at relatively high dose.	[99,100]
Chromogranin A and its cleaved products	Potentially involved in acinar cells migration, proliferation and differentiation during postnatal development; antifungal, antibacterial, antiparasitic,	[101,102]
Endothelin and Sarafotoxin	Growth factor, wound healing, assists in innervation, involved in saliva secretion	[103-105]
Galanin	Induce saliva secretion	[13]
Gastrin and Cholecystokinin	Induce protein and amylase secretion, anti-inflammation	[106]
PACAP and Glucagon	Invoke saliva/protein secretion, promote lumenization during salivary gland development	[14,107]
Leptin	Hyperleptinemia decreased saliva function and composition	[108]
Natriuretic peptides	Potentially regulates SG homeostasis through control electrolyte secretion/re-absorption, modulating autonomous nervous system and vasoconstriction/vasodilation.	[109]
Neurotensin	Capable to evoke the cytosolic K^{+} signalling	[110]
NPY	Stimulate protein release in the salivary glands	[18]
Nucleobindin	Capable to evoke the cytosolic Ca^{2+} signalling	[111]
Opioid	Induced hyposalivation, xerostomia, reduced saliva composition.	[17]
Orexin	Regulate feeding behavior, potentially control circadian rhythm of salivation	[16]
Resistin	Could involve in development of IR and local inflammation of Sjogren syndrome	[112]
Somastostatin	Induce protein secretion in salivary glands	[113]
Tachykinin	Stimulate saliva secretion	[19]

Neuropeptide Y (NPY) is a 36 amino acid peptide belong to the pancreatic polypeptide family, discovered from porcine hypothalamus since 1982 by Tatemoto [114]. NPY is synthesized from a 97 amino acid precursor named pre-pro-neuropeptide Y (preproNPY). This precursor was cleaved multiple times at the endoplasmic reticulum to generate the biologically active NPY1-36 (NPY) [115]. Most of NPY function came from its interaction with six G-protein coupled receptors: (Y1, Y2, Y3, Y4, Y5 and Y6). NPY is widely expressed in both central and nervous system, and plays critical role in regulating multiple physiological processes, including food consumption, cognitive behavior, immune response and neuroprotection [116]. In the concept of anti-aging, NPY overexpressed transgenic mice had longer lifespan than its littermate, partially through regulation of energy metabolism and calories restriction, which effect is diminished in NPY-deficient mice [117,118]. NPY also provides significant neuroprotective properties against multiple neurodegenerative diseases, including Parkinson's disease, Alzheimer's disease, Huntington's disease and Amyotrophic Lateral Sclerosis [20,116]. NPY can induce dopaminergic neurons viability by activation of AKT and MAPK pathway; ameliorate inflammation side effect by preventing accumulation of microglia and inhibit interleukin release from microglia; reverted Amyloid β-induced neurodegeneration in both in vivo and in vitro condition [119-121]. Furthermore, NPY supplementation can improve protein homeostasis either through upregulation of chaperones or by promoting autophagy pathways [122,123]. NPY possesses great therapeutic potential as an anti-aging and neuroprotective agents.

Substance P (SP), an 11-amino acid peptide, is a member of tachykinin neuropeptide family and was the first neuropeptide was discovered in history by von Euler and Gaddum in 1931. SP is synthesized from the precursor gene preprotachykinin-1 (TAC1) [124,125]. Through alternative splicing, 4 isoforms of TAC1 were produced: alpha, beta, gamma and delta. All of these isoforms can produce SP but beta and gamma isoforms can produce another

neuropeptide called neurokinin A (also known as Substance K) [125,126]. Similar to other neuropeptides, firstly the signal peptide is cleaved from preprotachykinin-1 to produce protachykinin-1; then protachykinin-1 got cleaved two more times to produce matured SP [126]. As the first discovered neuropeptide, effect of SP was studied exhaustively. SP is a recognized inflammatory modulator and a potent vasodilator [126]. SP is produced by peripheral nerves and immune cells in wounded tissue and subsequently attaches to its preferred receptors, NK1R, to regulate the wound-healing process through a series of events. [127]. As a vasodilator and a lymphocytes attractant, SP can enhance the delivery of lymphocytes to the injury sites, stimulate the production of cytokines from immune cells to create a pro-inflammatory microenvironment, which, in turn, induces the proliferation of endothelial cells and promotes angiogenesis [127-129]. Pro-wound healing effect of SP was also observed in the fibroblasts, cornea and intestine epithelial [130-132]. Additionally, several researches reported neurogenesis and neuroprotective effects of SP, suggested its high potential for further regeneration therapy [134,135].

2.8. Project aims and objectives

The aim of this project is (1) understanding of salivary gland dysfunction using aging-accelerated klotho knock-out mice model (2) to investigate potential roles of neuropeptides, such as NPY and SP in branching morphogenesis in embryonic salivary gland.

(1) Salivary gland dysfunction was well recorded in the postnatal development of aging-accelerated klotho knock-out mice model, however, there are limited studies about the impact of klotho deficiency toward embryonic salivary gland development. Several mice models overloaded with damage generated from primary hallmarks of aging exhibit both developmental defects and premature aging, therefore, we hypothesized that the salivary gland dysfunction in the klotho-deficient mice could originate at the developmental state, and used ex vivo culture method to analyze the embryonic development of salivary glands in this aging-accelerated model.

(2) Embryonic salivary gland development required a fine-tuning co-operation from epithelial, mesenchymal, neuronal, myoepithelial, lymphatic and endothelial cell population [1, 30]. Nervous system exhibits a multifront impacts toward salivary gland development, from maintaining the stemness of epithelial population through neurotransmitter Acetylcholine, regulating the acinar differentiation by Ngr1/Erbb3/mTor signaling and regulating the tubulogenesis through neuropeptide VIP [14,53,67, 135]. Despite the role of neuropeptides was studied exhaustively on matured salivary gland, there are limited research conducted to evaluate their potential impact on the salivary gland organogenesis. Therefore, organ culture system was applied to assess the possible influence of neuropeptide NPY or SP on embryonic salivary gland development.

III. MATERIALS AND METHOD

3.1. Compounds

The pan-FGFR inhibitor BGJ398 was purchased from Selleckchem (Houston, TX, USA). The MEK/ERK1/2 inhibitor U0126 was purchased from Promega (Madison, WI, USA). The neuropeptides NPY and SP were purchased from Tocris Bioscience (Bristol, UK). Acetylcholine chloride (Ach-A6625) was purchased from Sigma (St. Louis, MI, USA). Atropine sulfate (A10236) was purchased from Thermo (Waltham, MA, USA). These compounds were diluted directly into the organ culture medium below the membrane filter, while embryonic salivary glands were cultured on top.

3.2. Embryonic salivary gland isolation and culture

Mouse embryonic salivary glands were isolated at embryonic day 13.5 (E13.5). At E13.5, the uteri were removed from the timed pregnant mice and placed in ice-cold DMEM/F12 medium. The embryos were removed from their respective uteri using Dumont #5 forceps (Fine Science Tools, 11251 - 20). Embryos were placed in a 35-mm cell culture dish filled with 3 ml of PBS supplemented with P/S prior to salivary gland isolation. Under an Olympus SZ51 dissecting microscope (Olympus Corporation, Tokyo, Japan), the embryos were decapitated using Dumont #5 forceps. The embryonic tails were removed and placed in a 1.5 ml Eppendorf tube for genotype verification. The mandible and the tongue, which surround the salivary gland, were removed from the decapitated head by slicing the forceps across the mouth. The isolated mandible was subsequently placed on the cover of the 35-mm cell culture dish with the tongue facing down. Subsequently, the prongs of the forceps were slid into the space between the mandible and the tongue, and the midline of the mandible was sliced to expose the tongue and two salivary glands attached to the base of the tongue. After the surrounding tissues were removed, the glands were detached using forceps and collected in a 96-well plate on ice with 200 μl of

DMEM/F12 until all the embryos were dissected.

Isolated salivary glands were cultured on top of a 0.2 μm nucleopore track-etched membrane (Whatman, Maidstone, UK, and GVS, Italy) that floated on 1 ml of Organ Culturing Medium in the glass bottom area of the IVF culture dishes (Cat. No. 20260, SPL Life Sciences, Gyeonggi, South Korea) at 37 °C with 5% CO2. The organ culture medium used was DMEM/F-12 supplemented with 150 mg/mL ascorbic acid (Millipore-Sigma, St. Louis, MI, USA), 50 mg/mL holo-transferrin (Millipore-Sigma, St. Louis, MI, USA), and 1X Pen/Strep (100 units/mL penicillin, 100 mg/mL streptomycin; Thermo Fisher, Waltham, MA, USA).

For compound treatment, NPY, SP, and Ach were diluted in the media to a concentration of 100 nM. The dose of atropine (a cholinergic inhibitor) was 40 μM, while both BGJ398 and U0126 were used at a concentration of 10 μM. The media for embryonic organ culture were replaced every 24 h.

3.3. Genotyping of embryonic salivary gland tissue

We verified the genotypes of the isolated salivary gland samples by performing PCR using genomic DNA isolated from the embryonic tail. Two hundred microliters of tail lysis buffer (0.1 ml of 50 mM Tris (pH 8.0), 100 mM EDTA, 0.5% SDS, and 0.5 mg/ml proteinase K) was added to 1.5 ml Eppendorf tubes containing embryonic tail samples. The tubes were heated at 55 °C for 1 h to lyse the whole sample. Two hundred microliters of protein precipitation solution (Promega, Madison, WI, USA) was added to each tube, which was then centrifuged at 12000 rpm at room temperature (RT) for 5 min to pellet the protein. A total of 150 μl of supernatant was collected, and genomic DNA was precipitated by adding the same volume of ice-cold isopropanol. The mixture was then incubated on ice for 10 min, followed by centrifugation at 12000 rpm at RT for 5 min. The genomic DNA was washed with 400 μl of ice-cold ethanol (70%) prior to being diluted in 50 μl of DW. The concentration and quality of the isolated genomic DNA were determined using a NanoDrop spectrophotometer DS-11 (DeNovix, Wilmington, DE, USA).

Genotyping was performed using the polymerase chain reaction (PCR) with two pairs of primers containing a common forward primer and a specific reverse primer for the wild-type allele or the mutant allele. The expected amplification products were 815 bp and 419 bp for the wild-type and mutant strains, respectively. Detailed information about the genotyping primers is listed in Table 1. The PCR procedure was as follows: denaturation at 94 °C for 5 min; 30 cycles of 94 °C for 30 s, annealing at 66 °C for 30 s, and extension at 72 °C for 45 s; and a final extension at 72 °C for 10 min. The PCR products were loaded into 1% agarose gels and visualized under a UV lamp (SL-20, SeouLin Bioscience, Gyeonggi, Korea).

Table 2: Primers for genotyping.

Target	Sequences
Klotho WT	F: 5' - TTGTGGAGATTGGAAGTGGACGAAAGAG - 3' R: 5'- CTGGACCCCCTGAAGCTGGAGTTAC - 3'
Klotho MT	F: 5' - TTGTGGAGATTGGAAGTGGACGAAAGAG - 3' R: 5'- CGCCCCGACCGGAGCTGAGAGTA - 3'

3.4. Quantification of epithelial growth rate

Bright-field images of isolated embryonic salivary glands were collected every 24 h by an Olympus IX71 (Olympus Corporation, Tokyo, Japan) inverted microscope. The number of epithelial buds was counted using the image processing software FIJI. The epithelial growth rate was calculated as a Spooner ratio using the following equation:

The foldchange increase in the epithelial growth rate = the number of epithelial buds at 24 or 48 h ÷ the number of epithelial buds at 0 h.

3.5. qRT-PCR

Total RNA was isolated from the pooled embryonic salivary glands (up to 10 samples per condition) by utilizing the TaKaRa MiniBEST Universal RNA Extraction Kit (Takara Bio, Inc., Shiga, Japan) following the manufacturer's protocol. In brief, pooled embryonic salivary glands were lysed in 600 µl of extraction solution + 5% DTT by pipetting, and then, genomic DNA was removed by running the lysis solution through a gDNA Eraser Spin Column (provided by the manufacturer). Total RNA was precipitated by adding 70% EtOH to the flow-through mixture and then transferred to an RNA spin column (provided by the manufacturer). Total RNA was bound to the silica membrane in the RNA Spin Column and washed extensively to remove excess reagents. DNAse I was applied to remove remaining genomic DNA, after which the total RNA was eluted from the RNA spin column. The quality and concentration of total RNA were measured by a NanoDrop Spectrophotometer DS-11 (DeNovix,

Wilmington, DE, USA) to ensure that the A260/A280 ratio fell into a range between 1.8 and 2.1.

Total RNA was used as a template for quantitative real-time PCR (qRT PCR) using a GoTaq 1-Step RT qPCR System Kit (Promega, Madison, WI, USA) according to the manufacturer's protocol. The primers used for qRT PCR are listed in Table 1. Rps29 was used as a reference gene. PCR was carried out as follows: 1 cycle of 95 °C for 10 min; 40 cycles of 95 °C for 20 s, 60 °C for 20 s, and 72 °C for 20 s; and a melting curve beginning at 60 °C and increasing by 1 °C every 6 s, with SYBR green fluorescence measured at every interval. The PCR was performed on a qTOWER3 real-time PCR thermal cycler (Analytik Jena AG, Thuringia, Germany), and cycle threshold results were analyzed using qPCRsoft version 4.0 by Analytik Jena AG (Thuringia, Germany). Changes in gene expression were tested for statistical significance ($p < 0.05$) relative to the control by Student's t test.

Table 3: Primers for qRT-PCR.

Target	Sequences
Rps29	F: 5' - TCACCAGCAGCTCTACTGGAGT - 3' R: 5'- TGAAGCCTATGTCCTTCGCGTA - 3'
FGF1	F: 5' - GAAAGTGCGGGCGAAGTGTA- 3' R: 5'- CATTTGGTGTCTGCGAGCC- 3'
FGF7	F: 5' - GGCAAAGTGAAAGGGACCCA- 3' R: 5'- CAATCCTCATTGCATTCTTTCTTTG- 3'
FGF10	F: 5' - GTCAGCGGGACCAAGAATGA- 3' R: 5'- CGTTGTTAAACTCTTTTGAGCCA- 3'
FGFR2b	F: 5' - AAGGTTTACAGCGATGCCCA - 3' R: 5'- AGAGCCAGCACTTCTGCATT - 3'
Muc19	F: 5' - CTGGGTCTGGAAGTAGAAGTA- 3' R: 5'- TCTAAGCCACAGAAGGAGAT- 3'
Smgc	F: 5' - TGGCTCTGCAACACAACAGT- 3' R: 5'- GGCGAAAAGCTCCCAGGTAA- 3'
Dcpp1	F: 5' - CGAAACCTCTCAGCCAGACTTT- 3' R: 5'- AGTGCAGGAATGTTTTCCAACT- 3'
Mist1	F: 5' - GCTGACCGCCACCATACTTAC- 3' R: 5'- TGTGTAGAGTAGCGTTGCAGG- 3'
Krt5	F: 5' - CAACGTCAAGAAGCAGTGTGC- 3' R: 5'- CAGCTCTGTCAGCTTGTTTCTG- 3'
Krt14	F: 5' – GCAGCAGAACCAGGAGTACAA - 3' R: 5'- CGGTTGGTGGAGGTCACATCT - 3'
Krt15	F: 5' – ATTCTGGCTGCCACCATTGA - 3' R: 5'- GGGTCAGCTCATTCTCATACTTGA - 3'

3.6. RNA-seq and data analysis

Total RNA was isolated from the pooled embryonic salivary glands (up to 10 samples per condition) by utilizing the TaKaRa MiniBEST Universal RNA Extraction Kit (Takara Bio, Inc., Shiga, Japan) following the manufacturer's protocol. RNA quality was assessed by an Agilent 2100 bioanalyzer using an RNA 6000 Nano Chip (Agilent Technologies, Amstelveen, The Netherlands), and RNA quantification was performed using an ND-2000 spectrophotometer (Thermo Fisher, Waltham, MA, USA). Next, a QuantSeq 3' mRNA-seq Library Prep Kit (Lexogen, Vienna, Austria) was used to construct the library for sequencing following the manufacturer's protocol. In brief, 500 ng RNA was reverse transcribed with Oligo-dT primers. The RNA template was removed after cDNA synthesis was complete. A tagged double-stranded cDNA library was synthesized from the single-stranded cDNA with random primers containing an Illumina-compatible linker sequence. Magnetic beads were used to purify the double-stranded cDNA library, and then the cDNA library with adapters and barcodes was generated by another round of PCR and magnetic bead purification. High-throughput sequencing was performed as single-end 75-bp sequencing using an Illumina NextSeq 500 (Illumina, Inc., San Diego, CA, USA).

Data analysis of the QuantSeq 3' mRNA-seq reads was performed by aligning the reads using Bowtie2. Differentially expressed genes were determined based on counts from unique and multiple alignments using coverage in Bedtools. The read count (RC) data were processed using the TMM + CPM normalization method in the EdgeR package within R using Bioconductor. ExDEGA software from Ebiogen was used to analyze the RNA-seq data and generate the final figures.

3.7. Whole-mount immunofluorescence staining

Embryonic salivary gland samples were fixed by replacing the organ culture media below the membrane filter with an approximate volume of 10% neutral buffered formalin and then incubated at 4 °C overnight with gentle rocking. Samples were collected in a 12-well plate, washed with PBS (3 × 15 min), and permeabilized by incubating with PBSTx (PBS + 0.2% Triton X-100) for 1 h at RT with gentle rocking. Following permeabilization, the samples were blocked in 5% normal goat serum diluted in PBSTx for 1 h at RT with gentle rocking (300 µl solution per well). Then, the samples were incubated with primary antibodies diluted in PBSTx + 5% normal goat serum for 48 h at 4 °C with gentle rocking (300 µl solution per well). After the primary antibody incubation was complete, the samples were washed 3 × 15 min in PBSTx at RT with gentle rocking. After washing, the samples were incubated with labeled secondary antibodies and DAPI diluted in PBSTx + 5% normal goat serum for 48 h at 4 °C with gentle rocking (300 µl solution per well). Detailed information on the antibodies used is listed in Table 3. After 48 h of incubation, the samples were washed 3 × 15 min in PBS to remove all excess staining reagents prior to mounting.

Before mounting, the samples were submerged in 500 µl of PBS in a single well of a 12-well plate. The samples were transferred onto a glass microscope slide (Marienfeld Superior, Germany) by pipetting. Excess PBS was removed by pipetting and using paper towels. Forceps were used to separate the samples to circumvent contact. One hundred microliters of Malinol mounting solution (Muto Pure Chemical, Tokyo, Japan) was pipetted on top of the samples before a 22 × 22 mm thick, #1.5 coverslip (Marienfeld Superior, Germany) was placed on top. After all the samples were mounted, the microscope slides were placed in a dark container at RT for 24 h to allow the mounting media to solidify. The samples were subsequently analyzed by a Nikon Eclipse Ti A1 (Nikon, Tokyo, Japan) confocal microscope. Fluorescence images were acquired by z-stack imaging with a

3.0 μm step size and a 10X objective, unless otherwise stated. After the z-stack images were acquired, the final images were generated through maximum intensity Z-projection using NIS-Elements software from Nikon (Nikon, Tokyo, Japan).

3.8. Western Bloting

For Western blotting, total protein was isolated from the pooled embryonic salivary glands (up to 10 samples per condition). Embryonic salivary gland samples were collected in a 1.5 mL Eppendorf tube, and 200 μl of RIPA buffer containing 1 g/mL phosphatase inhibitor and protease inhibitor was added to the tube. The Eppendorf tubes were then placed in an ultrasonic bath for 5 min to lyse all the embryonic salivary gland tissues. The sample lysates were subjected to SDS PAGE and transferred to PVDF membranes (Millipore, Burlington, MA, USA), which were blocked with 5% skim milk for 2 h and incubated with primary antibodies diluted in TBST (TBS + 1% Tween 20) overnight at 4 °C with gentle rocking. The next day, the PVDF membranes were washed with TBST 3 times for 5 min before they were incubated with the appropriate secondary antibodies for 1 h at RT with gentle rocking. Detailed information on the antibodies used is listed in Table 3. The membranes were subsequently washed with TBST for 3 × 5 min, after which the protein concentration was detected via the chemiluminescence method. Briefly, the membrane was covered with a 1:1 mixture of Immobilon Western Chemiluminescent HRP Substrate (Millipore, Burlington, MA, USA), and protein signals were visualized using an Amersham ImageQuant 800 system (Amersham, UK).

Table 4: Antibodies for Western Blot and Immunofluorescence.

Antibodies	Manufacturer	Identifier
Mouse monoclonal TUBB3	Santacruz	sc-51670
Mouse monoclonal Actin	Santacruz	sc-47778
Mouse monoclonal FGF1	Santacruz	sc-55520
Mouse monoclonal FGF7	Santacruz	sc-365440
Mouse monoclonal AKT	Santacruz	sc-81434
Mouse monoclonal p-AKT	Santacruz	sc-293125
Rabbit polyclonal FGFR1	Abcam	ab137781
Rabbit polyclonal ERK1/2	Cell Signaling Technology	9102S
Rabbit polyclonal p-ERK1/2	Cell Signaling Technology	9101S
Rabbit monoclonal mTOR	Cell Signaling Technology	2983S
Rabbit polyclonal Aqp5	Cell Signaling Technology	59558S
Rabbit polyclonal p-p38	ProteinTech	28796-1-AP
Rabbit polyclonal ZO-1	ProteinTech	21773-1-AP
Rabbit polyclonal SOX2	ProteinTech	11064-1-AP
Rabbit polyclonal FGFR2	ProteinTech	13042-1-AP
Rabbit polyclonal KRT5	ProteinTech	28506-1-AP
Rabbit polyclonal KI67	ProteinTech	27309-1-AP
Mouse monoclonal p-mTOR	ProteinTech	67778-1-IG
Goat anti-mouse IgG, HRP conjugated	Promega	W401B
Goat anti-rabbit IgG, HRP conjugated	Promega	W402B
Goat anti-Mouse IgG, Alexa FluorTM 488	Invitrogen	A28175
Goat anti-Rabbit IgG, Alexa FluorTM 488	Invitrogen	A27034
Alexa FluorTM 594 goat anti-rabbit IgG	Invitrogen	A11012
Alexa FluorTM 594 goat anti-mouse IgG	Invitrogen	A11005

3.9. Short interference RNA (siRNA) transfection.

Predesigned siRNAs targeting murine FGFR1 (ID: 14182-1) and FGFR2 (ID: 14183-1) were purchased from Bioneer (Daejeon, Korea) and transfected into cultured embryonic salivary glands using Lipofectamine RNAiMAX reagent (Invitrogen, Waltham, MA, USA). One microliter of siRNA and 6 μl of Lipofectamine RNAiMAX were diluted in 100 μl of OptiMEM (Thermo Fisher, Waltham, MA, USA) separately; the mixture was mixed together and incubated at room temperature for 5 min. The final complexes were added to the organ culture medium below the floating membrane and were changed every 24 h. Embryonic organs were cultured with the siRNA complex for 48 h prior to downstream analysis.

3.10. Statistical analysis

All experimental results are presented as the mean ± SD of at least three independent experiments. Differences between groups were analyzed by multiple t-tests and ANOVA, followed with Bonferroni adjustment. Differences were considered significant at $p < 0.05$ (*$p < 0.05$, **$p < 0.01$, ***$p < 0.01$).

IV. RESULTS

4.1. Embryonic salivary gland development in aging accelerated Kl$^{-/-}$ mice

Salivary gland branching morphogenesis is a complex process that requires the cooperation of numerous signaling factors. We adapted *ex vivo* culture of embryonic salivary glands to adequately mimic this process and to analyze the morphogenesis of the salivary gland during organogenesis. As shown in Figure 1, the number of epithelial buds in the salivary glands was markedly lower in Kl-/- mice than in wild-type mice. Quantification of epithelial buds revealed that at the initial timepoint (E14), the wild type mice had a slightly greater number of epithelial buds than did the Kl-/- mouse samples. However, the difference in epithelial bud number between wild-type and Kl-/- embryonic salivary glands became more pronounced in a time-dependent manner. On E15, wild type had 44 % more epithelial buds than Kl-/- mice; and on E16; wild type mice showed a higher number of epithelial buds (approximately 62 %) than the Kl-/- mice (Figure 1B). Interestingly, the epithelial growth rate was not significantly different between wild type and Kl-/- mice (Figure 1C). The results of the immunofluorescence staining assay for the neuronal marker β-tubulin III revealed that the innervation of cholinergic neuronal cells in salivary glands were reduced in Kl-/- embryonic salivary glands compared to wild type salivary glands. At E16, expression of ZO-1, a marker of ductal differentiation, was also significantly reduced in the lumen of the main duct of the Kl-/- embryonic salivary gland (Figure 1D).

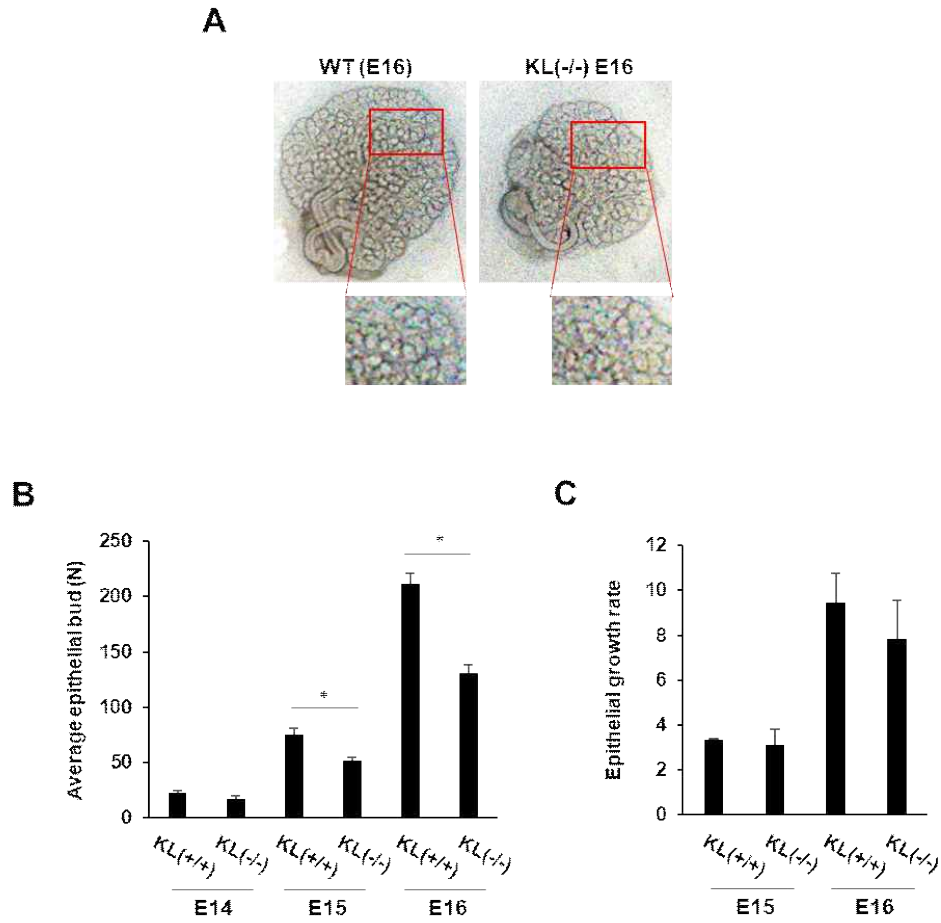

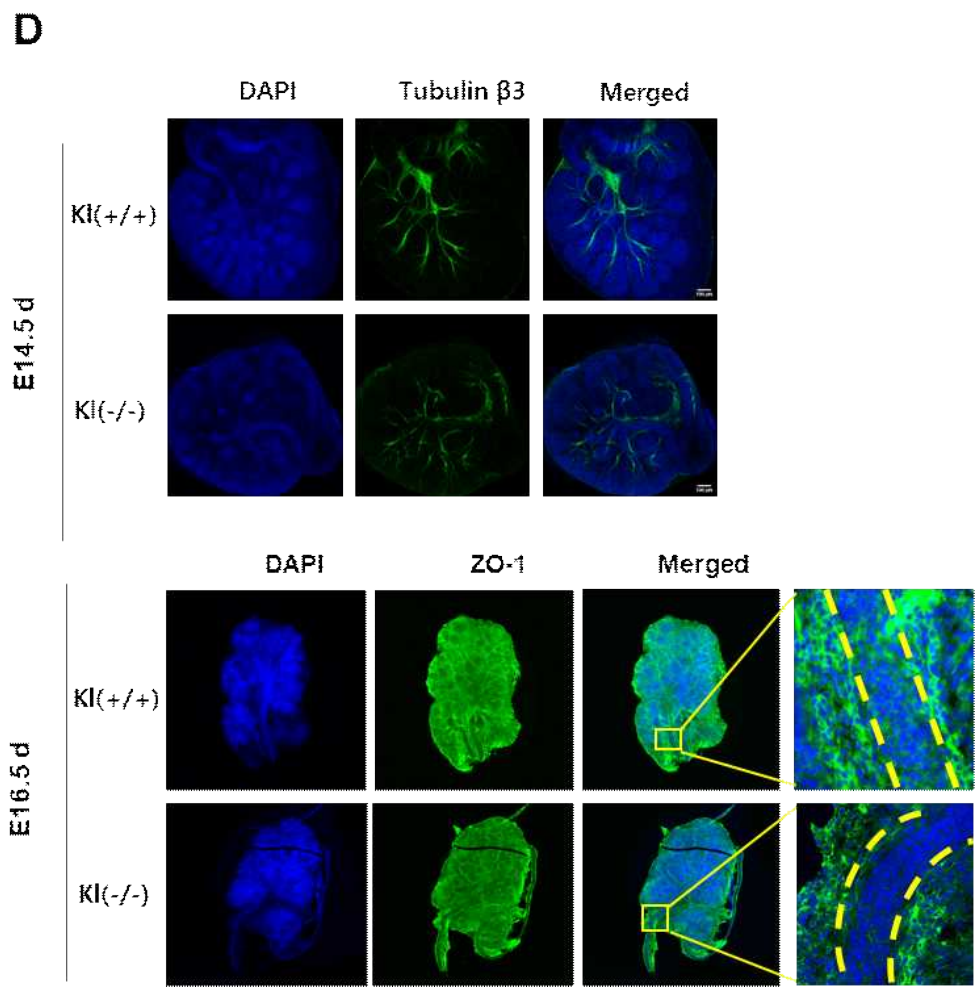

Figure 1. Lacking of klotho slightly altered salivary gland development *in vitro*.

Embryonic salivary glands from $Kl^{+/+}$ and $Kl^{-/-}$ mice were harvested at E13.5 and cultured *ex vivo* for 48 hours. Pictures were taken at the time of culture (0h) as the baseline and every 24 hours using an inverted microscope. Wholemount immunofluorescent staining against Tubb3 and Zo-1 were performed and pictures were taken by Nikon A1 Confocal Microscope (A). Brightfield images of $Kl^{+/+}$ and $Kl^{-/-}$ embryonic salivary glands at E16. (B-C). Quantification of number of epithelial buds per glands and epithelial growth rate (n = 3 glands per genotype; mean ± SD; Student's t test. $*p < 0.05$, $**p < 0.01$). (D). Immunofluorescence staining of parasympathetic nervous system marker Tubb3 from WT and KL MT embryonic salivary gland at E15. (E). Immunofluorescence staining of ductal marker ZO-1 from WT and KL MT embryonic salivary gland at E16.5.

4.2. Neuropeptides NPY and SP induces embryonic salivary gland branching morphogenesis

To examine the potential effect of neuropeptides in salivary gland branching morphogenesis, E12 Kl -/- embryonic salivary glands were isolated and cultured in the organ culture medium with supplement of either SP or NPY over 48 hours, to cover the pseudoglandular and canalicular stage of salivary gland organogenesis. Over 48 hours, treatment of SP significantly promoted the branching development of salivary gland, as demonstrated in the number of epithelial buds (Figure 2). On the other hand, treatment with NPY promoted a noticeable but not statistical difference in Kl -/- embryonic salivary glands. In detail, SP treatment increase bud numbers by approximately 3 times after 24 hours and 48 hours. From these results, we proposed that the neuropeptides SP/NPY could promote the branching morphogenesis in the embryonic salivary glands.

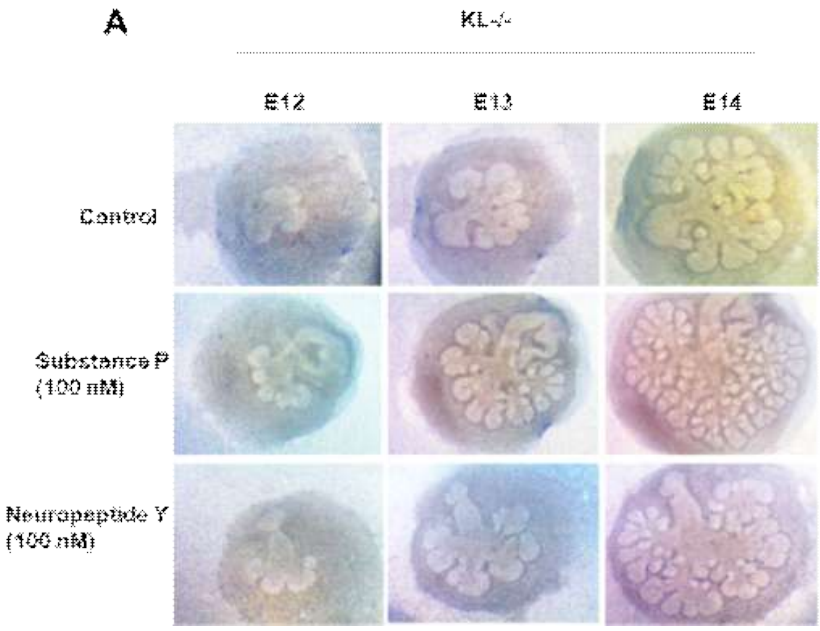

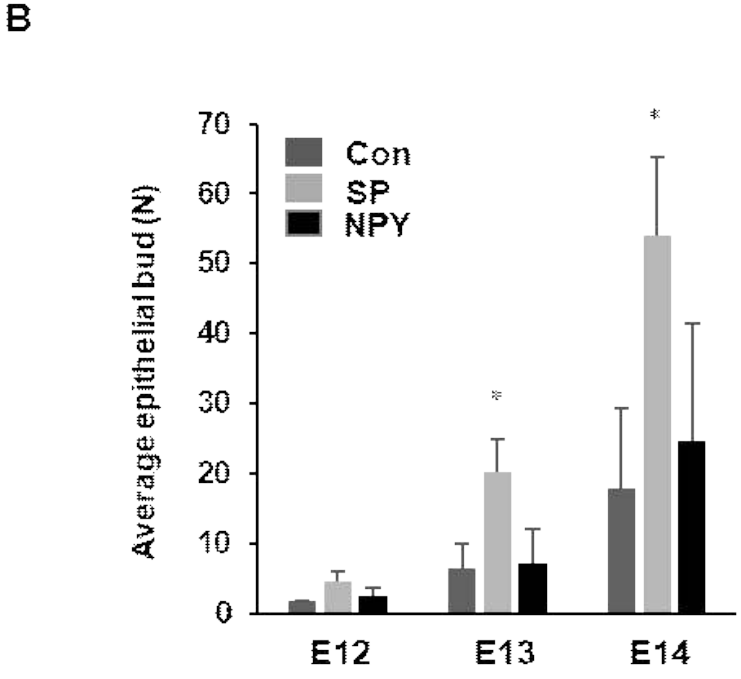

Figure 2. Neuropeptides SP and NPY induce branching morphogenesis in embryonic salivary gland from klotho -/- mice.

Embryonic salivary glands from $Kl^{-/-}$ mice were harvested at E12.5 and cultured *ex vivo* for 48 hours. 100 nM of neuropeptide SP/NPY was added to the culture media and refreshed for every 24 hours. Pictures were taken at the time of culture (0h) as the baseline and every 24 hours using an inverted microscope. (A) Brightfield images of $Kl^{+/+}$ and $Kl^{-/-}$ embryonic salivary glands after 48 hours of neuropeptide treatment. (B) Quantification of number of epithelial buds per glands. ($n = 3$ glands; $*p < 0.05$).

4.3. Neuropeptides SP and NPY induce branching morphogenesis in dependent of parasympathetic nervous system.

To examine potential signaling pathway induced by neuropeptide SP and NPY, we used the cholinergic inhibitor Atropine to evaluate effect of SP and NPY under the inhibition of parasympathetic nervous innervation in embryonic salivary glands. As demonstrated in figure 3A; cholinergic inhibition significantly abrogated salivary gland branching morphogenesis; however, supplementation of either neuropeptide SP or NPY can rescue Atropine-induced reduction of epithelial branching, as the quantification of number of epithelial buds were demonstrated in figure 3B. Confocal images of immunostaining with neuronal marker Tubb3 confirmed a reduction in parasympathetic innervation in Atropine-treated samples, which was rejuvenated in the presence of neuropeptide SP or NPY (figure 3C). These data suggested that Neuropeptide SP and NPY can induce the branching morphogenesis in dependent of parasympathetic nervous system.

A

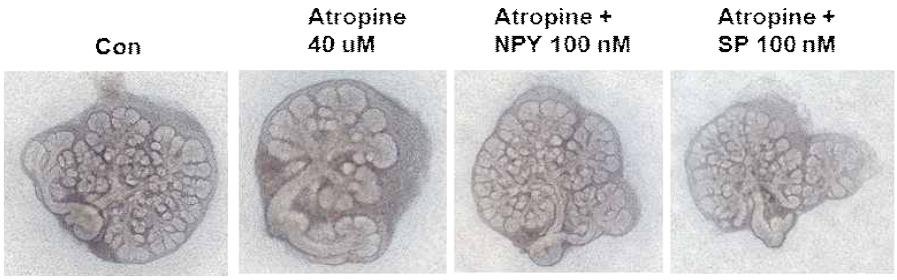

B

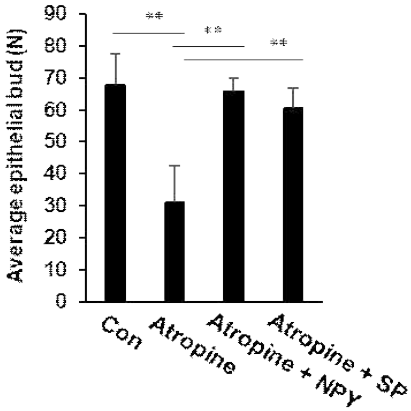

C

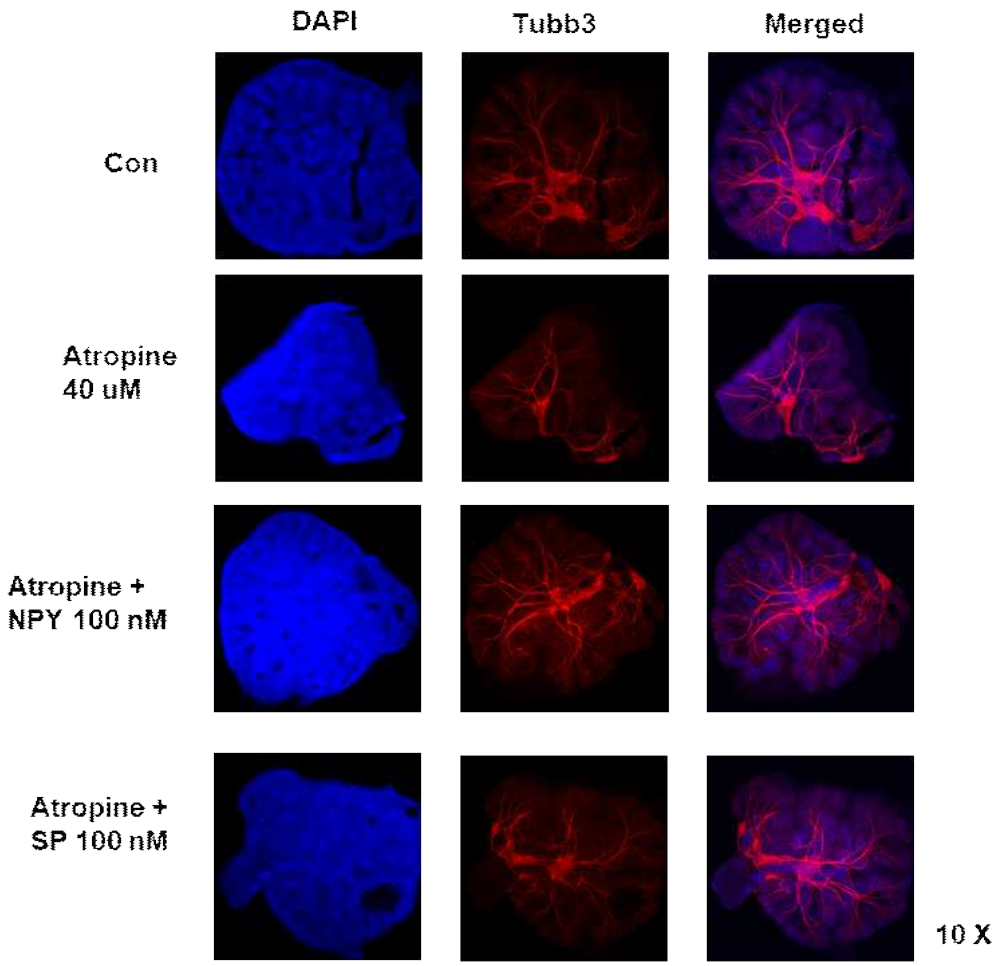

Figure 3. Neuropeptides SP and NPY induce branching morphogenesis in dependent of parasympathetic nervous system.

Embryonic salivary glands from $Kl^{+/+}$ mice were harvested at E12.5 and cultured ex vivo for 48 hours. 100 nM of neuropeptide SP/NPY and 40 μM of Atropine was added to the culture media and refreshed for every 24 hours. Pictures were taken at the time of culture (0h) as the baseline and every 24 hours using an inverted microscope. Wholemount immunofluorescent staining against Tubb3 were also performed and pictures were taken by Nikon A1 Confocal Microscope (A). Brightfield images of wild type embryonic salivary glands treated with neuropeptides SP/NPY with or without cholinergic inhibitor Atropine. (B). Quantification of number of epithelial buds per glands (n = 3 glands per group; mean ± SD; Student's t test. $**p < 0.01$, $***p < 0.001$) (C). Immunofluorescence staining of parasympathetic nervous system marker Tubb3 after 48 hours of treatment.

4.4. NPY and SP promote neurogenesis in the embryonic submandibular salivary glands.

To further confirm the involvement of neuropeptides NPY and SP in the branching morphogenesis; E13.5 embryonic salivary glands were harvested and treated with neuropeptides for 48 hours prior immunofluorescence staining against Sox2, a stem cells marker and a regulator of acinar development, and Tubb3, a marker for neuronal cell population. As demonstrated in Figure 4A; we found that the Sox2 expressed ubiquitously in the glands, and colocalized with the neuronal cells (Tubb3 stained). We also found that NPY or SP could induce the neurogenesis in embryonic submandibular salivary gland, as neuronal outgrowth with newly formed branches extended to peripheral buds and higher expression of Tubb3 was detected in the neuropeptide treated groups. Extensive neuronal network can be observed clearer in the higher magnification (Figure 4B). We concluded that treatment of NPY and SP induce the formation and branching of cholinergic nerves in the embryonic salivary gland.

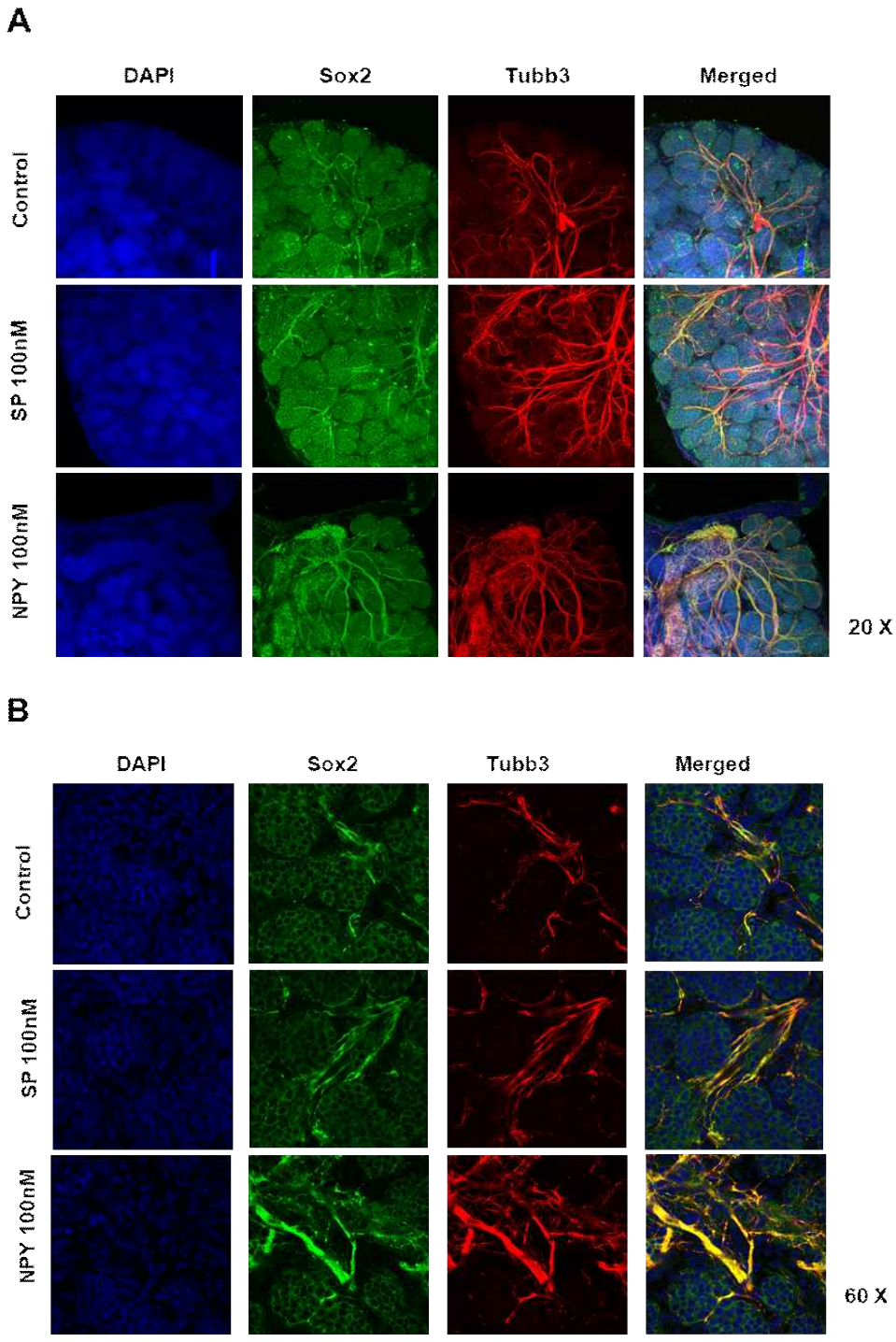

Figure 4. Neuropeptides SP and NPY promotes neurogenesis in embryonic salivary gland.

Embryonic salivary glands were harvested at E13.5 from $Kl^{+/+}$ and treated with 100 nM of SP/NPY for 48 hours (refresh media every 24 hours), prior staining with neural population markers (Tubb3) and Sox2 a stem cells marker and a regulator of acinar development. Picture were taken by Nikon A1 Confocal Microscope. Picture at 20X magnificent were Z-stack images, step size is 3 μm and final pictures were generated through Maximum Intensity Z-projection option in FIJI. (A) - 20X magnificent and (B) - 60X magnificent.

4.5. NPY and SP induces keratin expression and epithelial cell proliferation in embryonic salivary glands

Cytokeratin 5 (Krt5) and Cytokeratin 14 (Krt14) is one pair of intermediate filament proteins expressed at the basal layer of epithelium. This pair of proteins were established as the markers of the progenitor cells in the embryonic salivary glands. Cytokeratin 15 (Krt15) is a marker for both inner and outer ductal cells clusters in the embryonic salivary glands. mRNA expression of Krt5, Krt14 and Krt15 were upregulated after 48 hours of treatment with either NPY or SP (Figure 5A). qRT-PCR results of the marker for the basal epithelial layer Krt5 were verified by Immunofluorescence staining (Figure 5B). Staining with proliferation markers Ki67 verified that both neuropeptide NPY and SP induced cell proliferation effect at the peripheral epithelial buds (Figure 5C). Immunostaining with Krt14 verified that neuropeptide treatment induced higher expression of Krt14 at the peripheral area of the epithelial buds, compare with the control samples (Figure 5D-5E). Additionally, cyclin D1, a marker for cell cycle progression from G1 to S phase, were also upregulated after neuropeptide treatment. Finally, Figure 5F-5G verified the upregulation of Krt15, a marker for epithelial cells at the intermediate layer. Our staining results showed that Krt15-positives cells, localized mostly at the root of the main duct, and are upregulated after 48 hours of incubation with NPY/SP. These results suggested that these neuropeptides NPY and SP, could promote the epithelial cell proliferation in embryonic salivary glands.

A

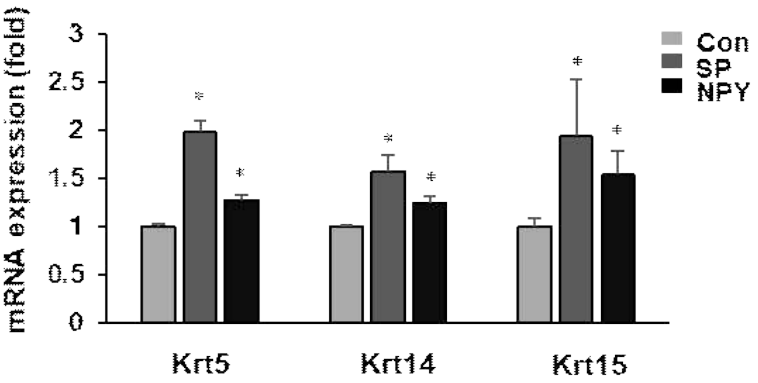

B

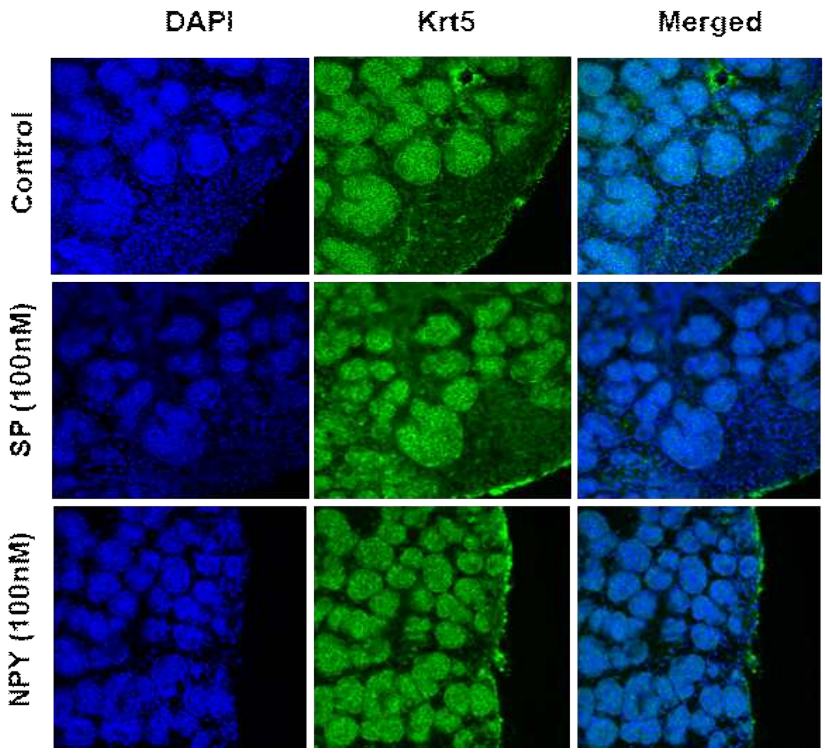

C

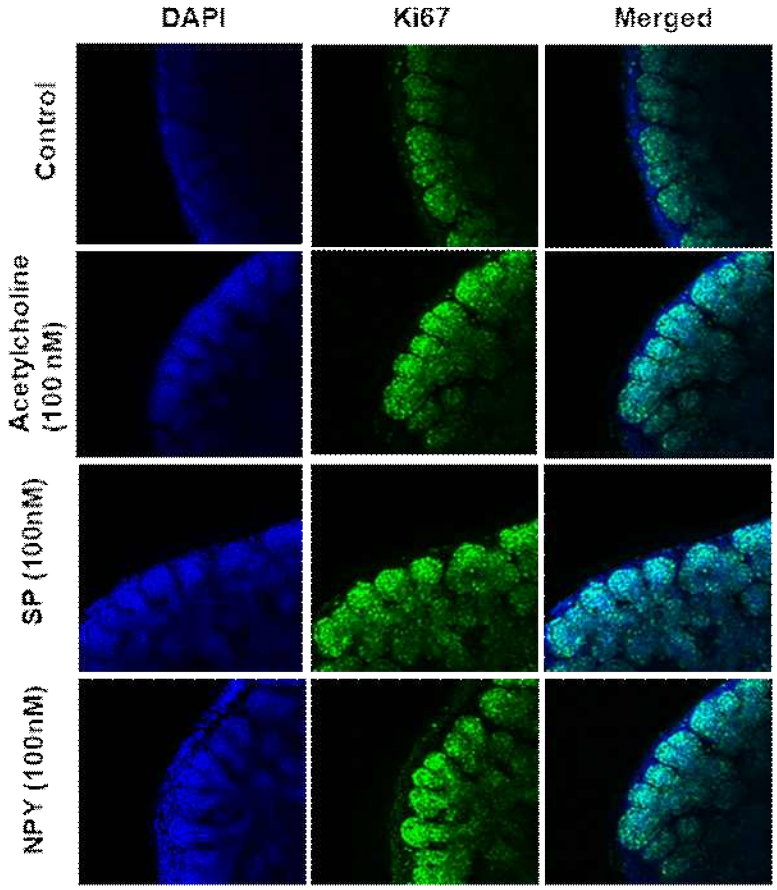

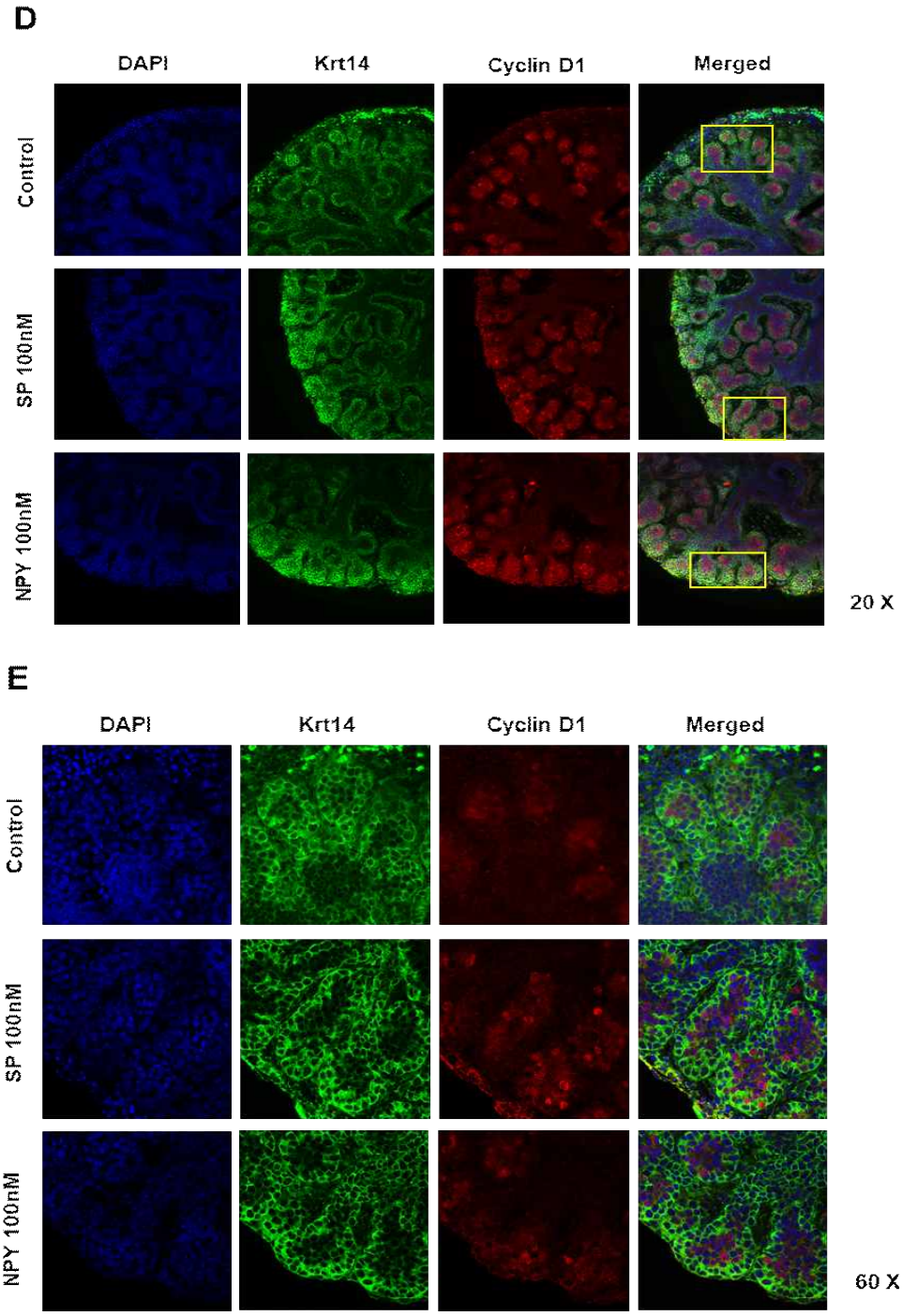

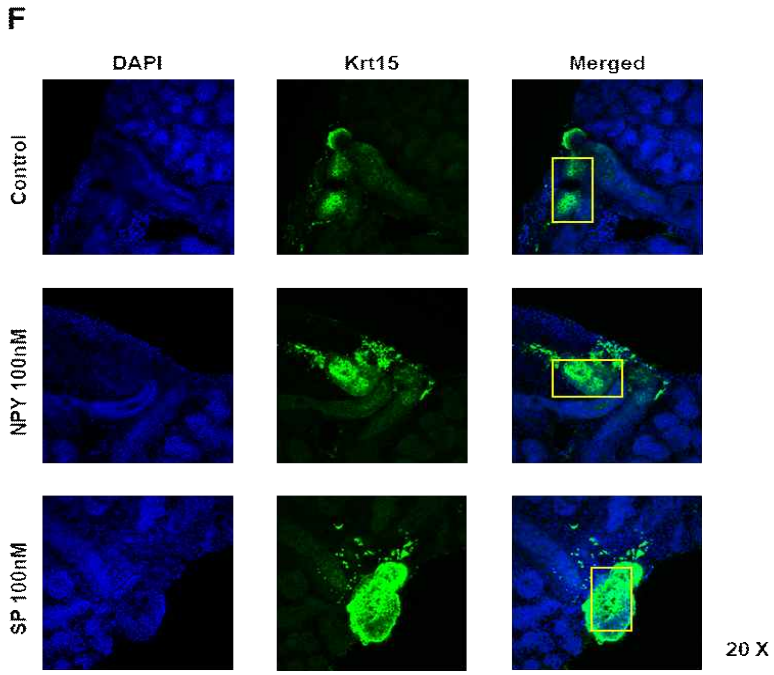

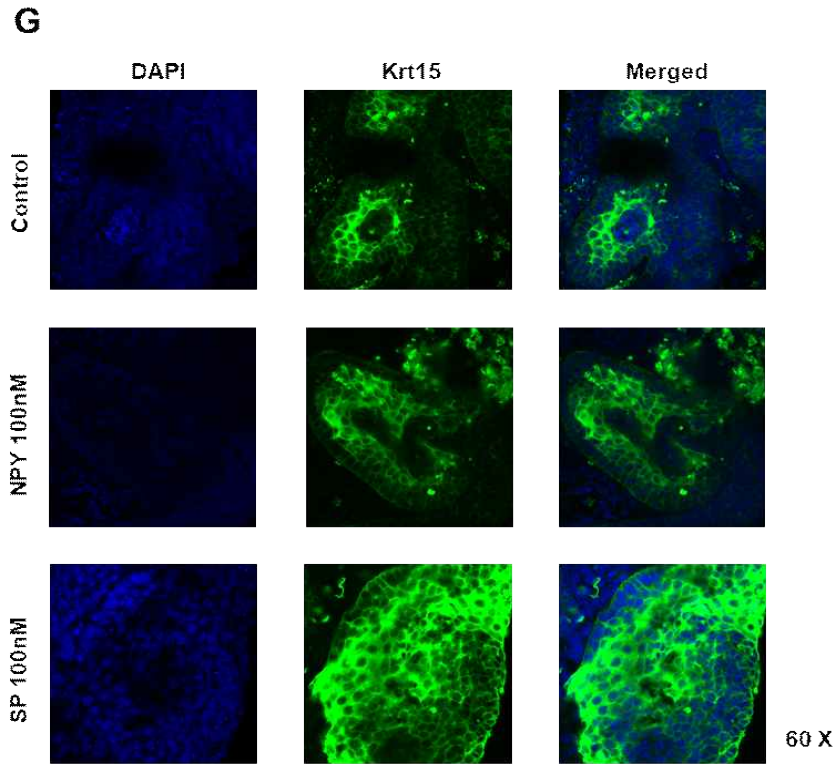

Figure 5. Neuropeptides SP and NPY promote epithelial cell proliferation in embryonic salivary gland.

Embryonic salivary glands were harvested at E13.5 from Kl+/+ and treated with 100 nM of SP/NPY for 48 hours (refresh media every 24 hours). Pooled glands were used to isolate total mRNA prior running qRT-PCR. Additionally, wholemount immunofluorescent staining against various epithelial markers and proliferation markers were conducted and pictures were taken by Nikon A1 Confocal Microscope (A). qRT-PCR analysis of Krt5/Krt14 and Krt15. Fold changes of gene expression are normalized to Rsp29. (n = 3; mean ± SD; Student's t test. $*p < 0.05$). (B). Immunofluorescence staining of Krt5 - marker for epithelial progenitors. (C). Immunofluorescence staining of Ki67 as an evaluation of cell proliferation. (D-E) Immunofluorescence staining of Krt14 -marker for basal epithelial and Cyclin D1 - markers for cell cycle. (D) - Pictures at 20X magnificent and (E) - Pictures at 60X magnificent. (F-G) Immunofluorescence staining of Krt15 - marker for intermediate epithelial. (F) - Pictures at 20X magnificent and (G) - Pictures at 60X magnificent.

4.6. NPY and SP induces salivary gland functional - related markers

To further investigate the potential effect of NPY and SP in the salivary gland development, E15.5 embryonic salivary glands were harvested and treated with neuropeptides for 48 hours. Then the samples were harvested and stained with the secretory protein AQP5 as the marker for acinar maturation, and tight junction protein ZO-1 as the marker for luminal development during the canalicular stage. Western blot was also conducted to determine the potential signaling pathway involved in neuropeptide treatment. As illustrated in figure 6A, AQP5 signal is upregulated after treatment with either SP or NPY. Similarly, Tight junction protein ZO-1 expression is upregulated in the ductal lumen of the salivary gland treated with NPY and the size of the lumen is broader than that of control. (Figure 6B). Western blot analysis verified the upregulation of AQP5 and ZO-1 in both SP and NPY-treated group; also demonstrated that treatment with neuropeptide induced the phosphorylation of mTOR and Akt; especially after treatment with NPY (figure 6C). These data suggested that neuropeptide NPY/SP could activated Akt/mTOR pathway, which lead to acinar maturation and ductal lumen expansion in embryonic salivary gland during the canalicular stage.

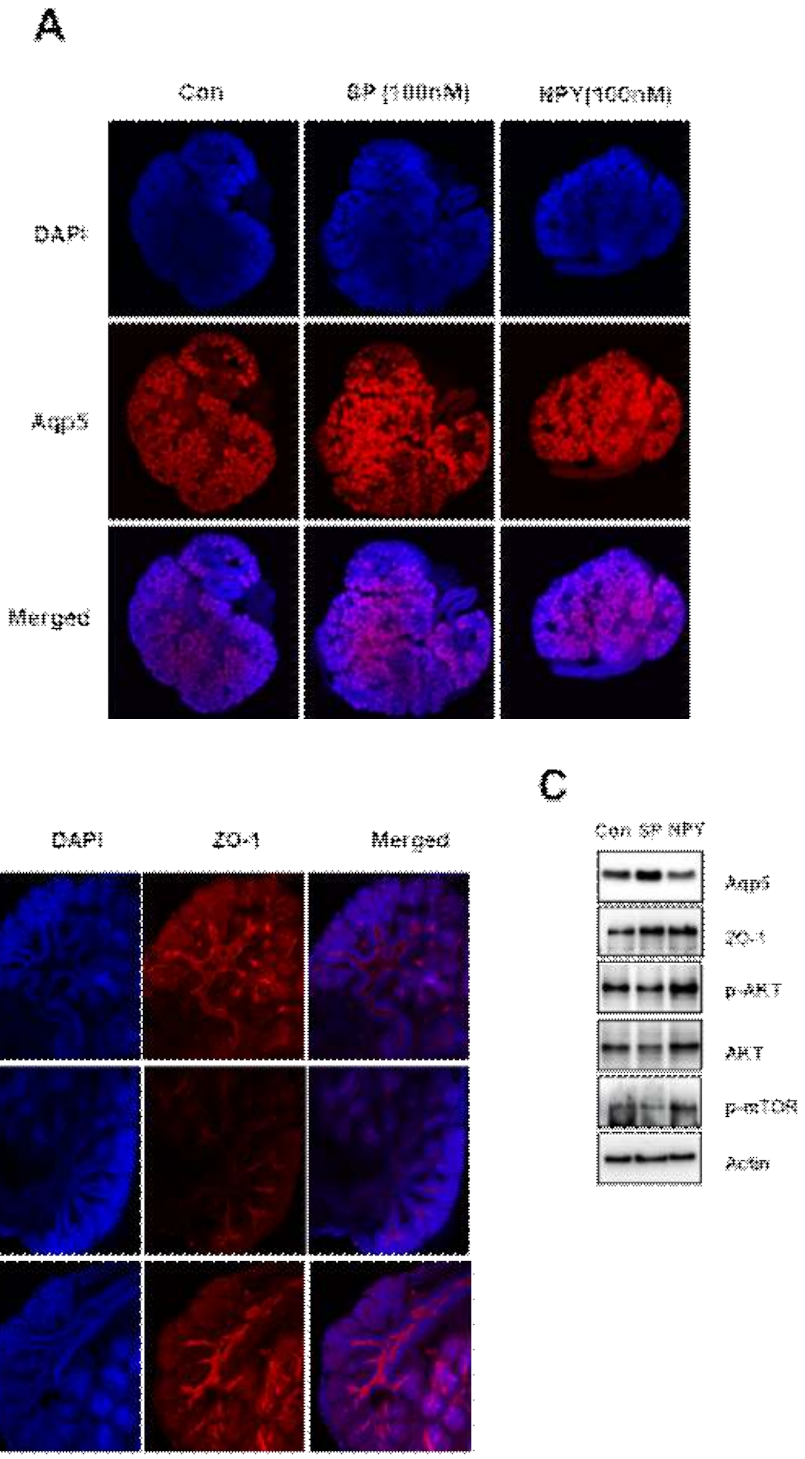

Figure 6. Neuropeptide SP and NPY promote ductal and acinar markers in embryonic salivary glands.

Embryonic salivary glands were harvested at E15.5 from $KI^{+/+}$ and treated with 100 nM of SP/NPY for 48 hours (refresh media every 24 hours). Pooled glands were used to isolate total protein prior running Western Blot. Additionally, wholemount immunofluorescent staining against ductal marker ZO-1 and acinar marker AQP5 were conducted and pictures were taken by Nikon A1 Confocal Microscope. (A-B) Immunofluorescence staining of secretory channel AQP5 and ductal markers ZO-1, presence in the acinar/lumen of the embryonic SMG. (C) Western Blot analysis of E17 embryonic salivary gland treated with corresponding neuropeptides.

4.7. Inhibition of ERK1/2 signaling pathway abrogated NPY/SP-induced branching morphogenesis

Previous literatures suggested that NPY and SP can both activate the ERK1/2 signaling pathway, therefore we conducted several experiments to evaluate impact of ERK1/2 signaling pathway to neuropeptide-induced epithelial branching morphogenesis. Western blot data (Figure 7A) illustrated that ERK1/2 signaling are activated after neuropeptides treatment at either early stage (pseudoglandular and canalicular stage) at late stage (acinar/lumen maturation). Co-treatment of either neuropeptides with ERK1/2 inhibitor U0126 completely negate the NPY/SP-induced branching morphogenesis (Figure 7B). In particular, the epithelial structures grew at a slower rate and peripheral buds stopped dividing, compare with other groups. Compare with the control, the epithelial growth rate in the neuropeptide treated group doubled after 24 hours and increased by 1.6 times after 48 hours. On the other hand, in the presence of ERK1/2 inhibitor U0126; the epithelial growth rate reduced by 66% after 24 hours and approximately 85% after 48 hours, compare with the neuropeptide-treated group (Figure 7C). Immunofluorescence staining with neuronal markers illustrated that the parasympathetic nervous system development is greatly downregulated in the presence of ERK1/2 inhibitor. In the neuropeptide-treated groups, nervous system expanded greatly to the peripheral buds, while in the inhibition group, the nervous system mostly localized around the main ducts and the formation of new nerve branches are significantly inhibited (Figure 7D). These data suggested that inhibition of the ERK1/2 signaling pathway can partially abrogate the neuropeptides-promoted branching morphogenesis in embryonic salivary gland.

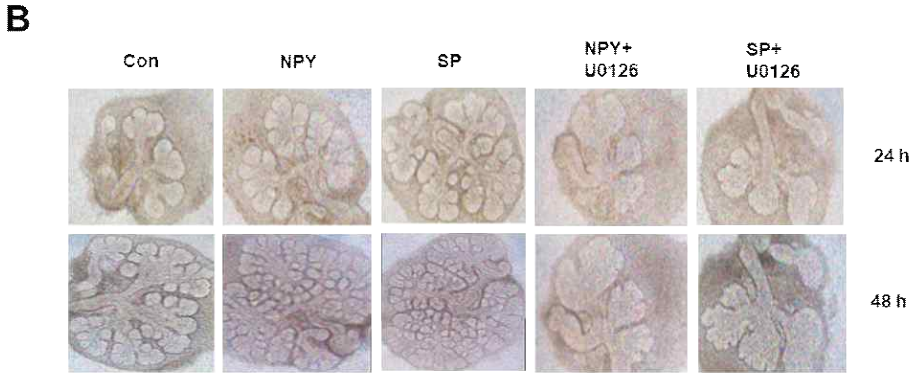

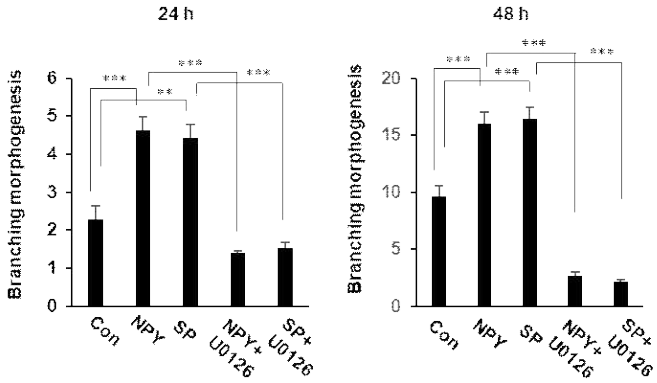

D

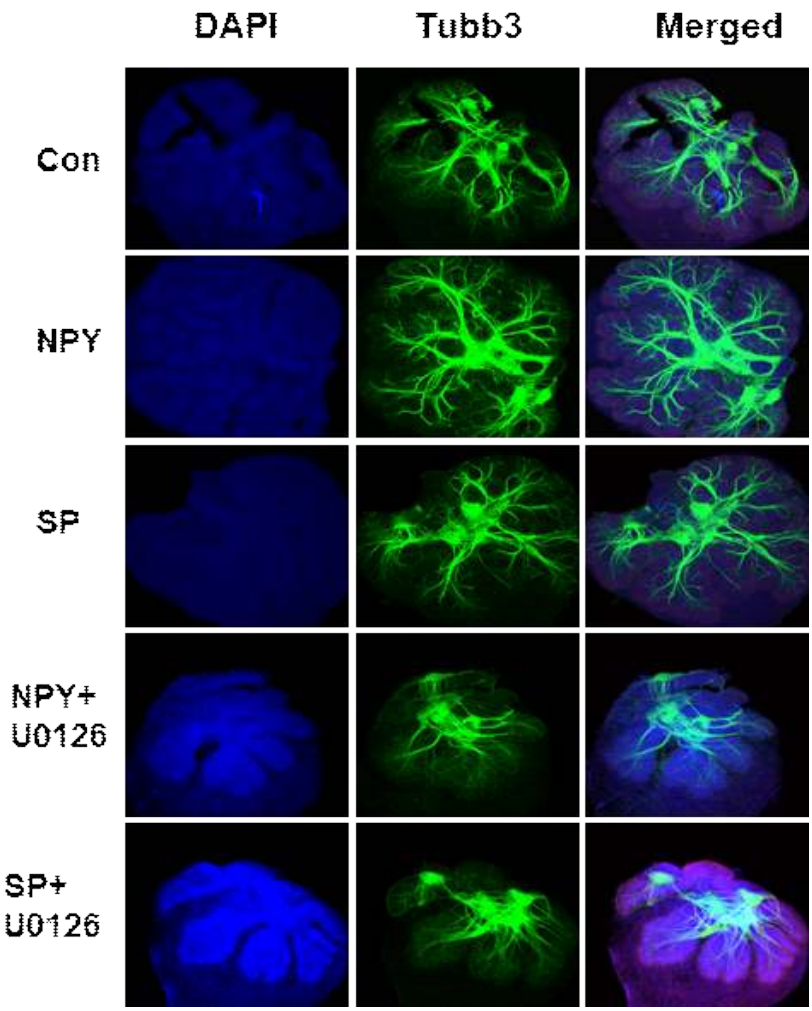

Figure 7. Inhibition of ERK signaling pathway abrogated neuropeptides-induced branching morphogenesis.

Embryonic salivary glands were harvested at E13.5 from $KI^{+/+}$ and treated with 100 nM of SP/NPY for 48 hours (refresh media every 24 hours). Pooled glands were used to isolate total protein prior running Western Blot. Additionally, wholemount immunofluorescent staining against neuronal marker TUBB3 were conducted and pictures were taken by Nikon A1 Confocal Microscope. (A). Western blot analysis demonstrated ERK1/2 is activated after treatment of SP and NPY at early and late stages of branching morphogenesis process. (B) Brightfield images of wild type embryonic salivary glands treated with neuropeptides SP/NPY with or without MAPK/ERK1/2 inhibitor U0126. (C) Quantification of epithelial growth rate (Spooner's ratio) after 24 hours and 48 hours of treatment. (D) Immunofluorescence staining of parasympathetic nervous system marker Tubb3.

4.8. RNA-sequencing analysis

We conducted a high through put screening with RNA-seq to identify the putative pathways induced by NPY and SP in the embryonic salivary glands. High purity mRNA was extracted from pooled samples of embryonic salivary glands treated with neuropeptides for 48 hours prior subjected for RNA-seq. Using z-score, the significantly changed genes were clustered into five different groups and visualized using heat map (Figure 8A). Venn diagram in figure 8B summarized the number of significantly up and down regulated genes after neuropeptide treatment (p-value < 0.05). In particular, NPY induced upregulation of 234 genes and downregulation of 320 genes. Those numbers of SP-treated group are 98 and 101 genes, respectively. Among all of these genes, 20 are co-upregulated, and 36 are co-down regulated by both NPY and SP (Figure 8B). Scatter plot in figure 8C-8D visualized the amount of differentially expressed genes. Detailed list of top 25 of down and up-regulated genes are listed in the Supplementary Table 1-4. We also conducted Gene Ontology enrichment analysis to identify the dominant biological process (BP) among the DEGs in NPY-treated and SP-treated group. In the SP-treated group, nervous system development, intracellular signal transduction and phosphorylation are the BP that has highest number of DEGs involved. In the NPY-treated group, the BPs that have highest number of DEGs are cell cycle, protein ubiquitination and apoptotic process (Figure 8E-8F).

A

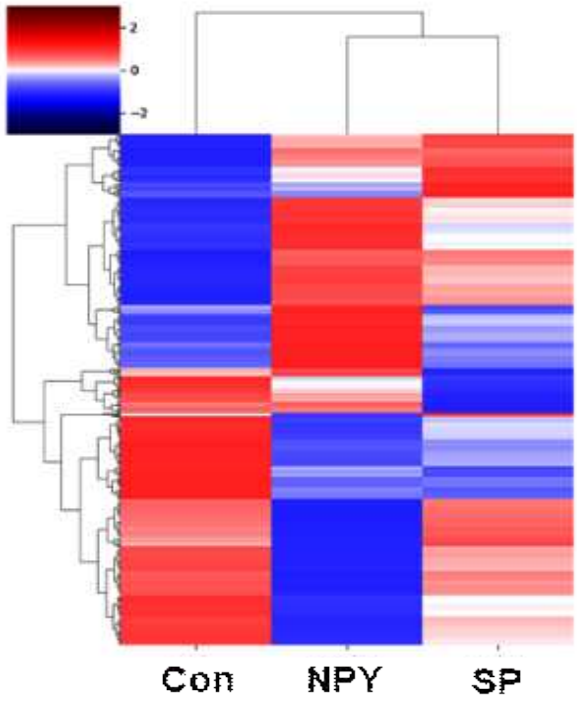

B

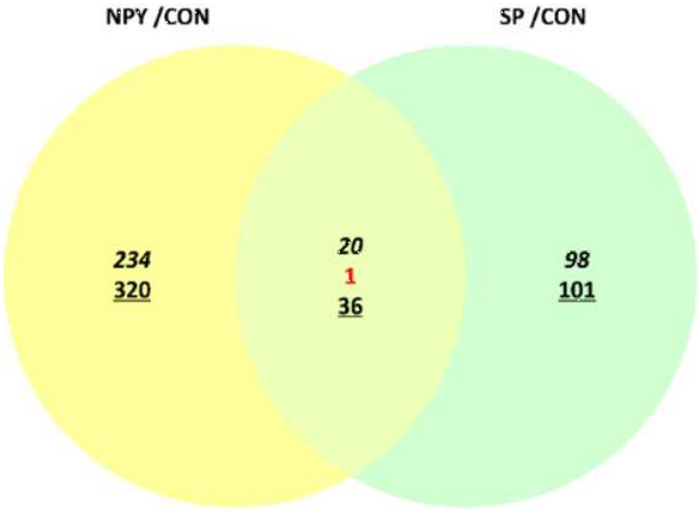

C

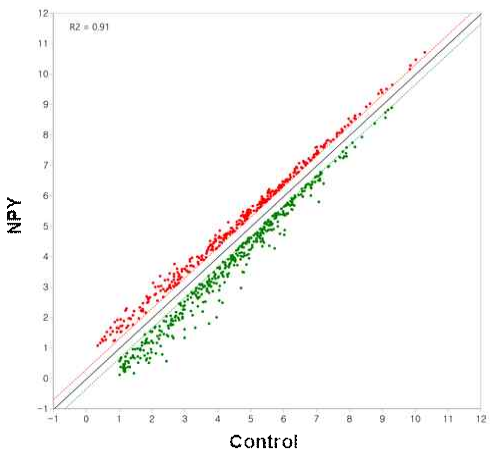

D

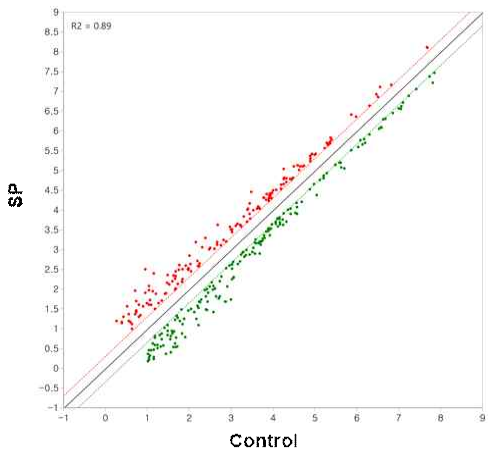

E

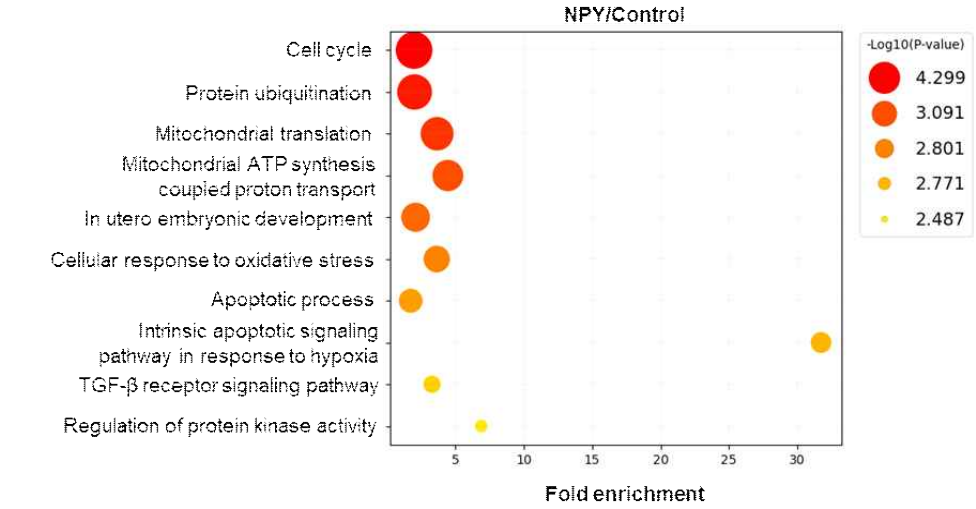

F

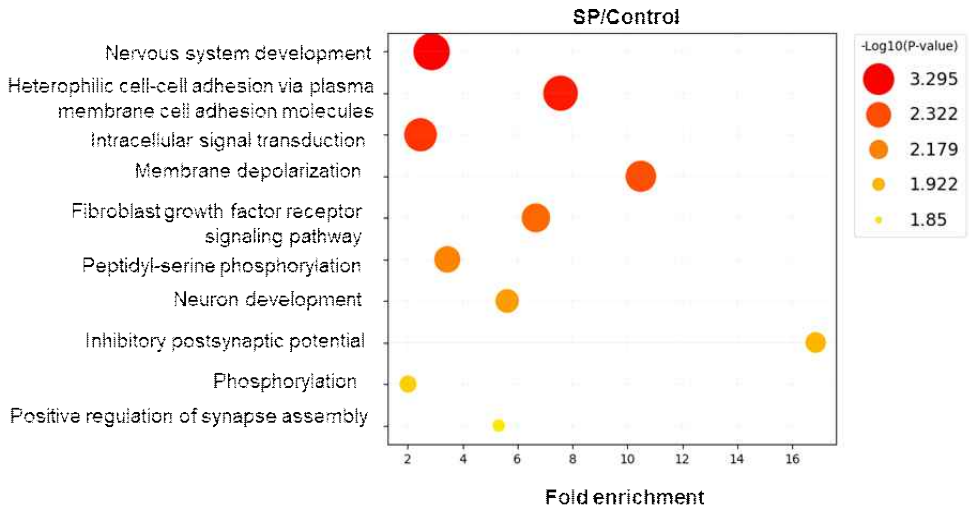

Figure 8. RNA-seq profiling from the wild type embryonic SMG treated with neuropeptides for 48 hours.

Embryonic salivary glands were harvested at E13.5 from $KI^{+/+}$ and treated with 100 nM of SP/NPY for 48 hours (refresh media every 24 hours). 10 glands were pooled in to one treatment group prior isolation of total mRNA. QuantSeq were conducted to evaluate gene expression. (A) Clustering heatmaps displaying differential expression genes (DEGs) between Control and neuropeptide-treated group. (B) Venn diagrams illustrated number of DEGs in NPY and SP-treated group. (C-D) Scatter plot demonstrated number of DEGs in NPY and SP-treated group. (E-F) GO enrichment analysis for biological process (BP) between SP-treated group and NPY-treated group versus control samples; generated from DAVID database. All figures were generated from ExDEGA software of Ebiogen.

4.9. NPY and SP regulates salivary gland branching morphogenesis through FGFR/AKT/mTOR/ERK1/2 signaling pathway.

We used qRT-PCR to evaluate the expression of NPY and SP-specific receptors in the embryonic salivary gland. Interestingly, qRT-PCR results showed that neither receptors are upregulated after neuropeptide treatment (Supplement data); similar to RNA-seq raw read data (data not shown); suggested a potential non-canonical signaling pathway in which NPY and SP regulated the branching morphogenesis. From RNA-seq data, we found several genes belong to fibroblast growth factors signaling pathway are significantly up-regulated; including Fgf1; Fgfbp1 and Cnpy2 as well as several markers for acinar differentiation, including secretory genes Muc19, Smgc, Dcpp1 and transcription factor Mist1. We decided to co-treat the neuropeptide with the pan-inhibitor of Fgf receptors BGJ398 to examine the potential connection between Fgf signaling and neuropeptide-induced branching morphogenesis.

Firstly, we used qRT-PCR to verify the RNA-seq results. mRNA expression of Fgf1, Fgf7 and Fgfr2b are upregulated after 48 hours treatment of either SP or NPY, but totally inhibited in the presence of BGJ398 (Figure 9A-9B). Similarity, the upregulation of secretory markers Muc19, Smgc, Dcpp1 and secretory transcription factor Mist1 after neuropeptide treatment was confirmed; and their expression is down-regulated significantly after inhibition of Fgf receptor signaling pathway.

We also examined impact of BGJ398 on branching morphogenesis, which is illustrated in figure 10. Pharmaceutically inhibition of Fgf receptors obstructed the growth of the embryonic salivary gland completely, even with the presence of neuropeptides SP or NPY. Peripheral buds lost the round shape and the formation of new buds is totally abrogated (Figure 10A). Quantification of epithelial growth rate showed that co-treatment of BGJ398 with neuropeptides reduced the Spooner's ratio by 70% after 24 hours and by

90% after 48 hours, compared with the neuropeptide-treated group only (Figure 10B). Western blot was conducted to examined the expression of several protein in the Fgf family and the canonical downstream pathway of the Fgf signaling. These data showed that Fgfr1 and Fgfr2b, two receptors that expressed mostly in the epithelial structures, are upregulated after treatment with the neuropeptide SP or NPY, as well as two ligands Fgf1 and Fgf7. Additionally, several canonical downstream pathways of the Fgfr signaling, including Akt/mTor, Erk, p38 also activated after neuropeptide treatment. Moreover, protein level of acinar secretory marker Aqp5 and lumen structure marker ZO-1 are also induced by SP or NPY treatment. Inhibition of Fgf receptors by BGJ398 completely reverted the upregulation of all these genes (Figure 10C).

Finally, we used siRNA against either Fgfr1 or Fgfr2, two most important receptors in the embryonic salivary glands, to evaluate their role in neuropeptide-induced branching morphogenesis. As demonstrated in Figure 11, E13.5 embryonic samples were cotreated with total four combinations of neuropeptides and siRNAs. Knockdown on single Fgf receptor does not alter the morphology of embryonic salivary glands in a remarkable manner, compared with the treatment of BGJ398 (Figure 11A). Quantification of branching morphogenesis through Spooner's ratio demonstrated that inhibition of any single Fgf receptors will decrease the neuropeptide-induced epithelial growth rate to the baseline level of control group, suggest that an intact Fgf receptor signaling system are required for the SP or NPY - induced branching morphogenesis (Figure 11B).

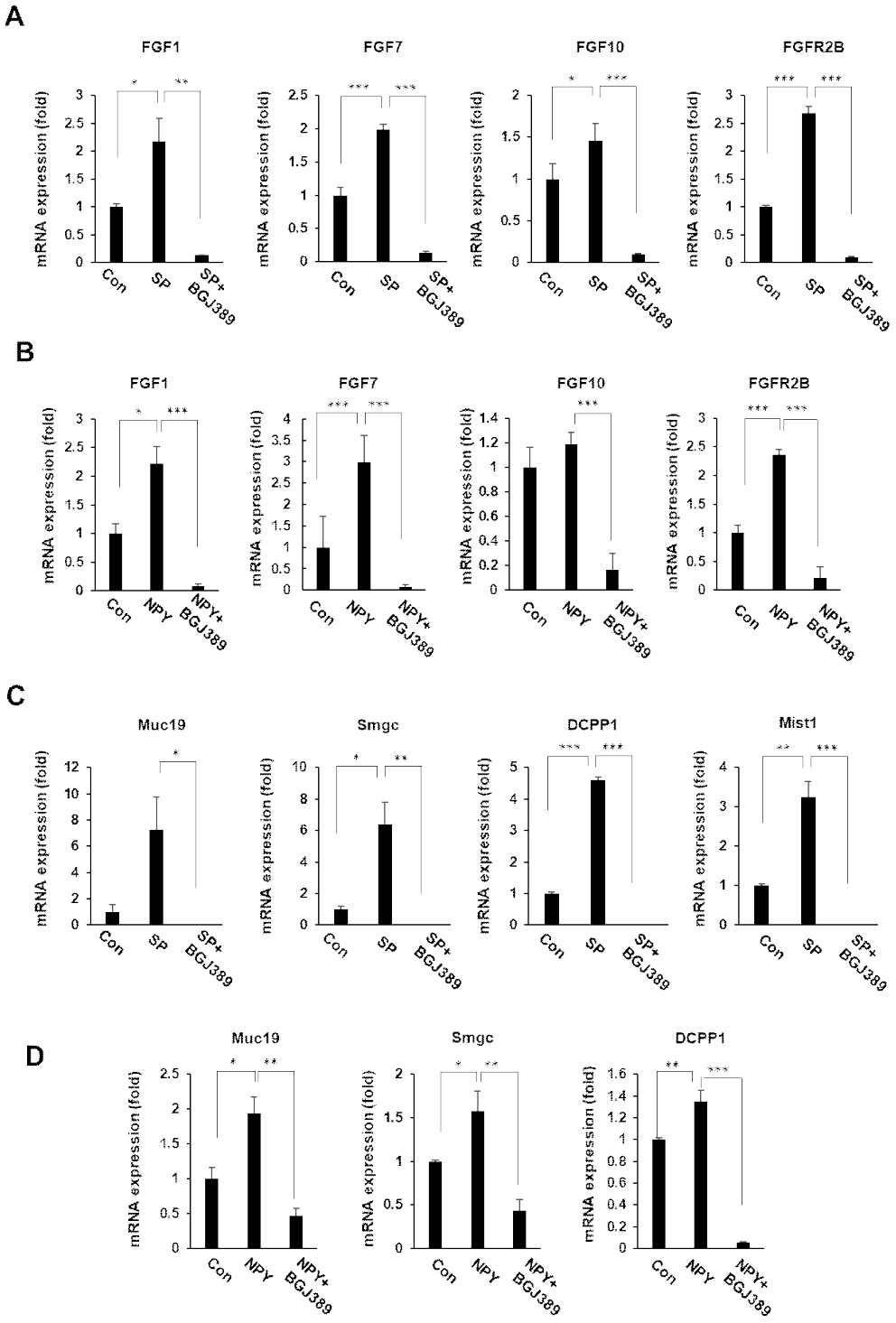

Figure 9. SP/NPY activated FGF signaling pathway and acinar secretory markers, but treatment with FGF receptors inhibitor BGJ389 inhibited its expression.

Embryonic salivary glands from $Kl^{+/+}$ mice were harvested at E13.5 and cultured ex vivo for 48 hours. 100 nM of neuropeptide SP/NPY and 1 μM of BGJ389 was added to the culture media and refreshed for every 24 hours. Pooled glands were used to isolate total mRNA prior running qRT-PCR. (A-B) qRT-PCR analysis of FGF signaling candidates mRNA expression in presence of SP/NPY (C-D) qRT-PCR analysis of acinar secretory markers mRNA expression in presence of SP/NPY. (n = 3; mean ± SD; Student's t test. $**p < 0.01$, $***p < 0.001$)

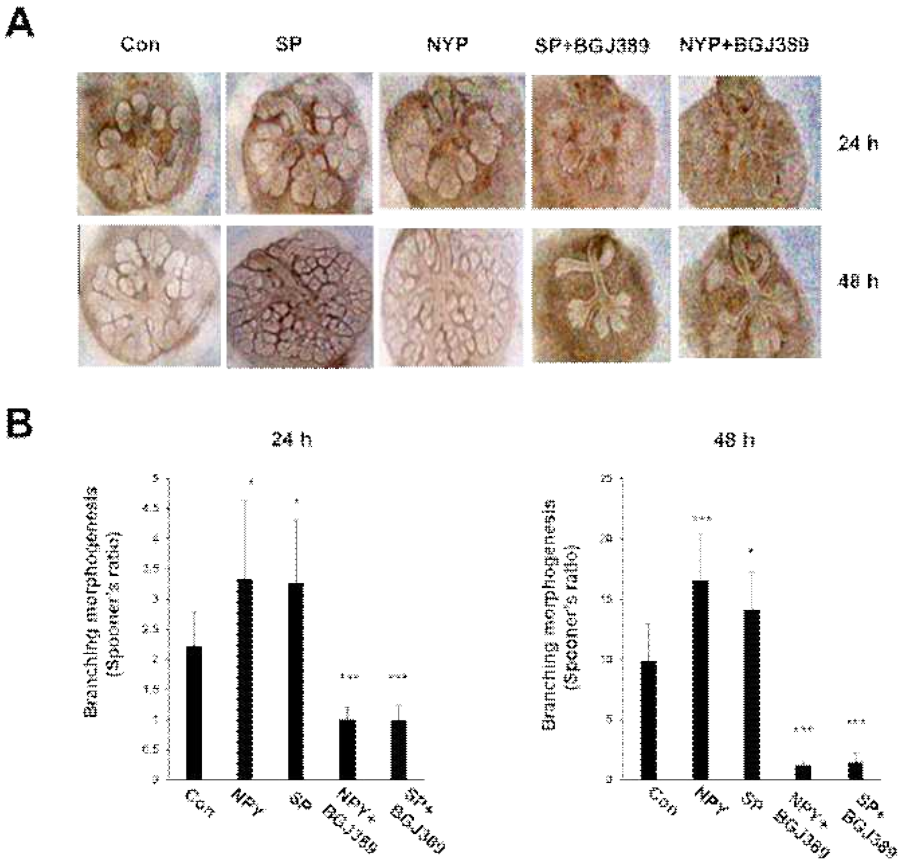

C

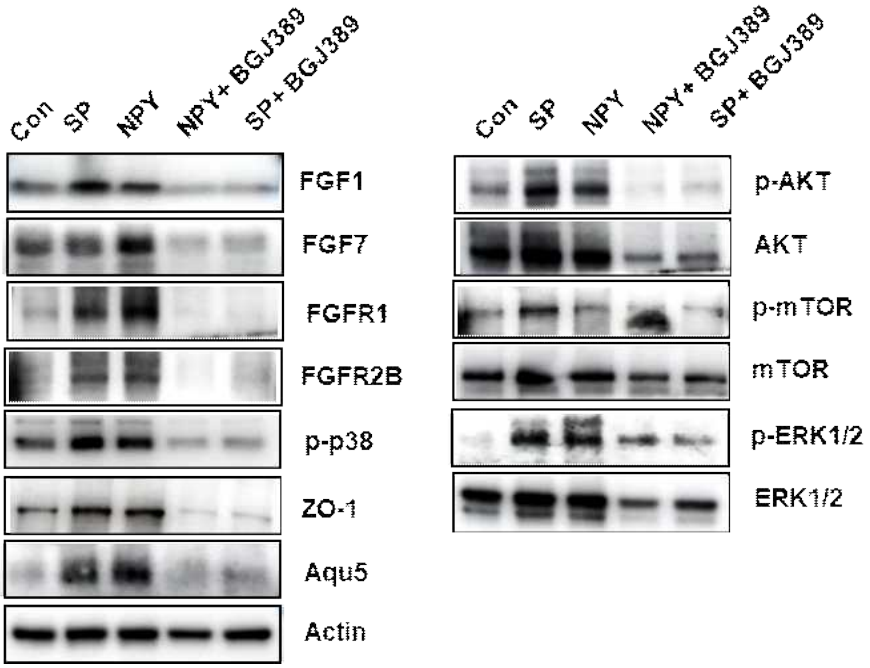

Figure 10. Inhibition of FGF receptors signaling abrogated neuropeptides-induced branching morphogenesis.

Embryonic salivary glands from $KI^{+/+}$ mice were harvested at E13.5 and cultured ex vivo for 48 hours. 100 nM of neuropeptide SP/NPY and 1 μM of BGJ389 was added to the culture media and refreshed for every 24 hours. Pooled glands were used to isolate total mRNA prior running Western Blot. Pictures were taken at the time of culture (0h) as the baseline and every 24 hours using an inverted microscope. (A) Brightfield images of wild type embryonic salivary glands treated with neuropeptides SP/NPY with or without FGF receptors inhibitor BGJ389. (B) Quantification of epithelial growth rate (Spooner's ratio) after 24 hours and 48 hours of treatment. (n = 6 glands/group; mean ± SD; Student's t test. $**p < 0.01$, $***p < 0.001$) (C) Western Blot analysis of FGF signaling and its canonical downstream pathway, as well as ductal and acinar markers.

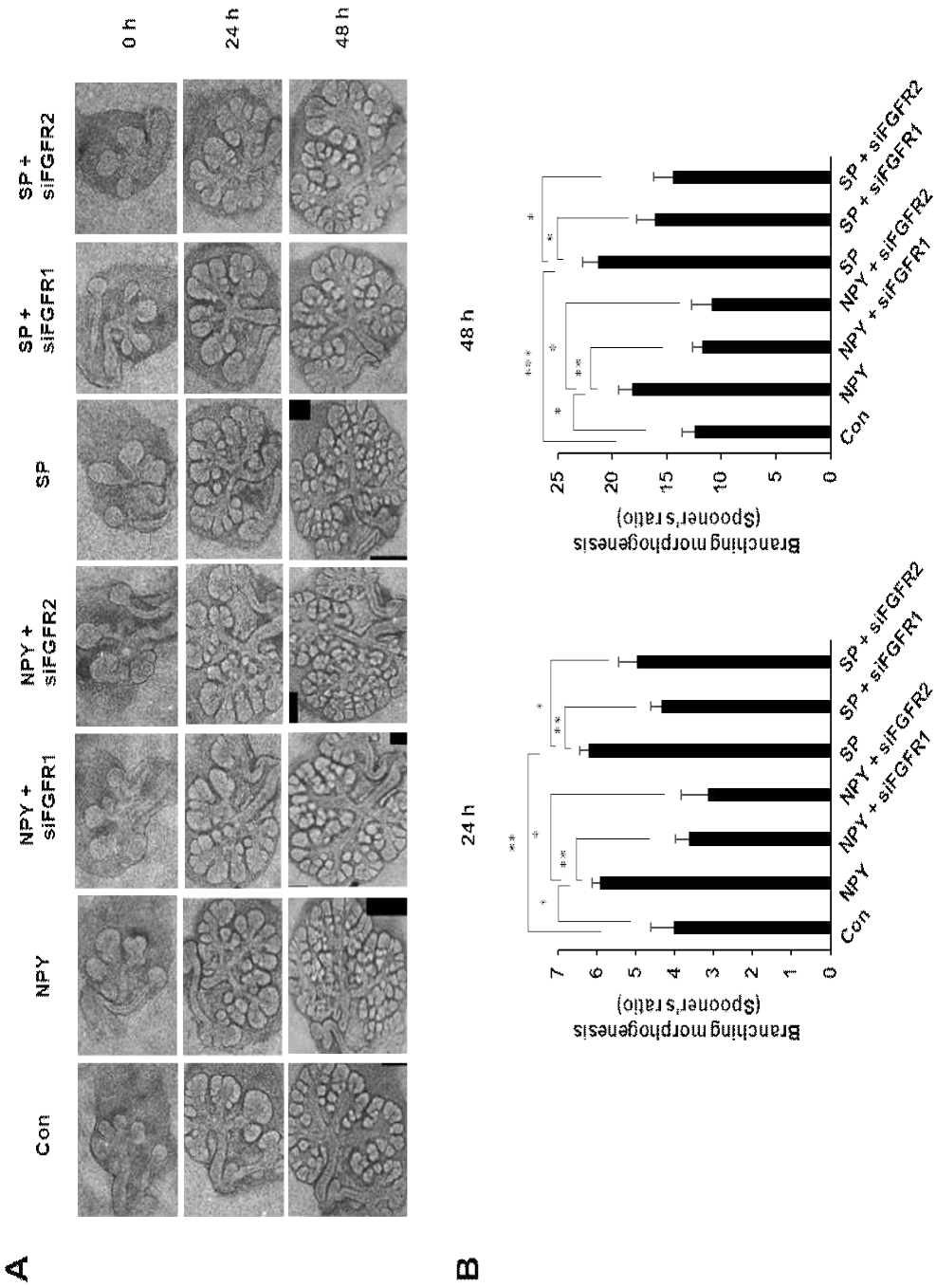

Figure 11. Inhibition of FGF receptors signaling abrogated neuropeptides-induced branching morphogenesis.

Embryonic salivary glands from $KI^{+/+}$ mice were harvested at E13.5 and cultured ex vivo for 48 hours. 100 nM of neuropeptide SP/NPY and 1 μM of siRNA target either FGFR1 or FGFR2 was added to the culture media and refreshed for every 24 hours. Pooled glands were used to isolate total mRNA prior running Western Blot. Pictures were taken at the time of culture (0h) as the baseline and every 24 hours using an inverted microscope. (A) Brightfield images of wild type embryonic salivary glands treated with neuropeptides SP/NPY with or without FGF receptors inhibitor BGJ389. (B) Quantification of epithelial growth rate (Spooner's ratio) after 24 hours and 48 hours of treatment. (n = 4 glands/group; mean ± SD; Student's t test. ∗∗p < 0.01, ∗∗∗p < 0.001)

V. DISCUSSION

With the exception of a few outlier species, such as *Turritopsis dohrnii*, which appears to defy aging, and *Proteus anguinus*, notable for their extraordinarily long lifespans, it is largely accepted that aging is an intrinsic and universal process that eventually leads to death [136]. Surprisingly, numerous ideas have developed to explain the mechanics of aging and how they interlink aging with the complicated developmental processes that occur throughout an organism's existence. These developmental phases, which include embryogenesis, histogenesis, and organogenesis, involve finely coordinated spatiotemporal changes in genetic expression that are regulated by complex molecular pathways.

Interestingly, several evidences illustrated that these hallmarks of aging can impede embryogenesis. A compelling illustration of this connection is exemplified in the Atr-Seckle mouse model, featuring mutated alleles of the ATR gene—a homologous counterpart to the human ATR gene. This model manifests accelerated aging phenotypes coupled with developmental defects, including dwarfism, osteoporosis, a shortened lifespan, and a notable increase in DNA damage within embryos, subsequently resulting in reduced embryo size [137]. Similarly, during the embryonic and neonatal phases, there are observable decreases in body and organ growth in the Cdc42GAP-deficient mouse model, which is characterized by increased Cdc42 activity. These physiological changes include a shorter life expectancy, decreased body mass, osteoporosis, muscular atrophy, and kyphosis, which are probably caused by the surge of cellular senescence [138,139]. Additionally, animals lacking Smarca6 activity make a strong argument since they show extensive demethylation and an increase in senescence markers. These mice experience a variety of early aging symptoms, such as graying hair, a shortened lifespan, cachexia, and kyphosis [140]. Together, these modified mouse models demonstrate a strong relationship, highlighting the possibility that the main causes of damage linked to aging characteristics may interfere with organ development, resulting in organ atrophy

and functional deterioration in the postnatal period.

Klotho is one of the most recognized aging-suppressing gene over the last three decades, which is capable of extending life expectancy of mice through a variable of mechanism, including anti-oxidative stress, anti-senescence, maintain metabolic homeostasis, and regulation of numerous signaling pathway [77,85-90]. The development of aging-resembled phenotypes in klotho-deficient mice was attributed to the dysfunction of phosphate, vitamin D and calcium metabolism, with the disruption in Klotho/FGF23/FGFR1 signaling axis [78,79]. $kl^{-/-}$ mice exhibit hyposalivation, reduced gland size, decreased connective tissue, and fewer granular ducts and serous acini compared to normal mice [7,8]. Additionally, the expression of various growth factors, ion pumps, and water channels involved in salivary gland function are also downregulated. Further investigations have demonstrated that multiple metabolic pathways crucial for salivary gland function, including acetylcholine biosynthesis, ascorbic acid biosynthesis, and the glutathione pathway, are disrupted in $kl^{-/-}$ mice [8-11]. However, these are limited studies using klotho-deficient mice as a model to studies the organogenesis during embryonic development, especially toward salivary glands.

In our data, the embryonic salivary glands isolated from klotho-deficient mice went through developmental process normally and did not suffered any significant alteration in overall structures, beside a small reduction of developed epithelial number (Figure 1A-B). Immunostaining revealed a small reduction in the expression of neuronal markers Tubb3 and ductal marker ZO-1 in the lumen of the main ducts. The reduction of neuronal population in embryonic salivary gland is consistent with previous report, in which $kl^{-/-}$ mice exhibits multiple neuronal-related defects, including behavioral impairments, synaptic loss, hypomyelination, and neuroinflammation [6,141,142]. It was reported that klotho supplementation triggered redox system to reduce neuronal death [143]. Tight junction protein ZO-1 is an epithelial marker and a scaffold protein that regulates the movement of ions between endothelial and epithelial cells. ZO-1

expression increased with the expanding of lumen, therefore it was used as a ductal marker during the embryonic development, together with Krt19 [14,144]. We also observed the reduction of Zo-1 in the salivary gland of $kl^{-/-}$ mice, compare with the wildtype littermates. Although we didn't conduct further analysis to investigate how klotho deficiency could lead to disruption in the cell-cell adhesion, multiple research reported Zo-1 and cadherin/catenin complexes expression is reduced under excessive oxidative stress, which is prevalence in the $kl^{-/-}$ mice [145]. However, the embryonic salivary glands of $kl^{-/-}$ mice are fully capable of develop into ductal and epithelial bud structure, as showing in Figure 1, suggest a possible compensatory mechanism against klotho deficiency. Further researches are required to fully elucidate the difference in the molecular mechanism in the salivary gland organogenesis in $kl^{-/-}$ mice, as well as its connection with the aging-induced dysfunction during postnatal development.

Neuropeptides, small proteins produced by neurons that exert their effects through G protein-coupled receptors, have a pervasive presence within the central nervous system [12,91]. Despite the absence of NPY and SP in mice leading to several physiological alterations, both TAC1-knockout mice and NPY-knockout mice exhibit normal viability, fertility, and normal organ morphology. Specifically, NPY deficiency in mice has been linked to increased bone mass, alterations in several behavioral activities, and reduced body weight, while TAC1-knockout mice exhibit atypical pain thresholds, heightened resistance to Kainate-induced neurotoxicity, and compromised bone quality [146-149]. Our data illustrated that neuropeptides NPY/SP could promote branching morphogenesis in klotho mutant embryonic samples (Figure 2), suggested their impacts in salivary gland organogenesis. Previously data also showed that NPY facilitated the bud formation in embryonic kidney through GDNF signaling [150]. In the context of embryonic salivary gland development, the interplay between neurons and epithelial cells assumes a pivotal role. This cross-talk governs essential aspects of salivary gland organogenesis,

encompassing the maintenance and proliferation of pluripotent epithelial cells, the processes of lumenization and ductal development, and the specification of secretory acini [14,52,53,67]. Prior investigations revealed several neuronal proteins that regulate salivary gland organogenesis, including NRTN, NRG1 and VIP. VIP, which regulates lumenization through its receptor VIP1R and the downstream cAMP/PKA signaling pathway, is the only neuropeptide. Our data expand the potential involvement of neuropeptides NPY and SP in the development of epithelial organs, then continued to investigate the deeper cellular and molecular mechanism of how NPY and SP could regulate the embryonic organ development.

Branching morphogenesis can be stimulated through multiple conditions, including neuronal, epithelial, endothelial, and cell-adhesion modulation. Inhibition of nervous signals reduced branching morphogenesis in the salivary gland greatly [53, 135]. Brightfield images illustrated that the neuropeptide SP/NPY can promote branching morphogenesis even when parasympathetic signaling is inhibited by atropine (Figures 3A - 3B). Atropine is an antagonist against the muscarinic receptors, which block acetylcholine signaling in the parasympathetic nervous system. Immunostaining showed that SP/NPY induces the recovery of the neuronal cells, thus rejuvenating the salivary branching morphogenesis (Figure 3C). Neurogenesis and the neuroprotective effects of both SP and NPY were extensively recorded. SP treatment boosted the proliferation of the neural stem cells, induced neural differentiation and accelerated recovery after ischemic injury [133,151]. NPY promotes neurogenesis in the dentate gyrus of the hippocampus through its receptor NPY1R and also the ERK1/2 signaling pathway in both in vitro and in vivo conditions [152]. NPY also facilitated neural revitalization after injury in multiple disease models, including Parkinson's and Alzheimer's diseases [119, 121]. Immunofluorescence staining also verified that treatment with neuropeptides promotes neural branching and the formation of new branches toward the peripheral epithelial bud (Figure 4). Together with an increase in neurons, Sox2 is found to colocalize within the

nervous system and be expressed higher in the outermost area of peripheral buds (Figure 4). In the concept of salivary gland organogenesis, Sox2 is a crucial factor. Losing Sox2 significantly reduced the number of epithelial buds and prevented the development of acinar cells, while overexpression of Sox2 can rejuvenate salivary gland tissues that underwent irradiation injuries [153,154]. Sox2-induced recovery and development are dependent on the parasympathetic nervous system; therefore, it is possible that neuropeptide NPY/SP supplementation could induce Sox2 expression in embryonic salivary glands by promoting neurogenesis in a cholinergic-independent manner. Furthermore, it is well recorded that aging induced a reduction and reorganization of innervation architecture in the salivary glands [155]. Artificial denervation leading to acinar atrophy an hyposalivation, but reinnervation induced the salivary gland endogenous regeneration [156]. A recently-developed drug-releasing hydrogel, which stimulate parasympathetic nervous system directly, promotes the endogenous regeneration of irradiated acinar and repopulates the irradiated salivary glands with functional secretory machines [157]. Therefore, inducing neurogenesis could be a potential method to recover the aging-induced salivary gland dysfunction. Our results demonstrated the significant potential of the neuropeptides SP and NPY in promoting neurogenesis and aiding nervous system recovery, offering promising avenues for regenerative therapies.

Cytokeratin are structural protein for cytoskeletal intermediate filaments, mainly expressed in the epithelial cells. In the embryonic salivary glands, In the embryonic salivary glands, Krt14 and Krt5 positive cells are progenitors of ductal and acinar cells, while Krt15 marked the epithelia population at the intermediate layer [57, 158]. Our research findings illuminate the influence of neuropeptides NPY/SP on cytokeratin expression patterns. Through (qRT-PCR), we observed significant upregulation of Krt14, Krt5, and Krt15 after exposure to NPY/SP (Figure 5). Subsequent analysis using confocal imaging revealed heightened Krt15 expression along the apical membrane of the ductal epithelium, forming the lumen, while Krt14 exhibited a shift toward the peripheral buds

following neuropeptide treatment. This intriguing observation aligns with the known influence of acetylcholine, indicating that stimulation from the nervous system via the cholinergic signaling pathway is imperative for pluripotent epithelial cell repopulation.

mTOR/AKT signaling pathway is a well-known regulator of cell proliferation and cell cycle; which functioned through two complexes mTORC1 and mTORC2. Inhibition of mTOR signaling pathway reduced the branching morphogenesis of salivary gland *in vitro* and *in vivo* [159]. Inhibition of mTORC2 complex prevented the development of secretory acini, which was regulated through a neuronal-epithelial crosstalk between NGR1-ERBB3 signaling [67]. Our data suggested that these neuropeptides (NPY and SP) could promote the expression of salivary glands functional markers at later stage of salivary gland development, including ZO-1 and AQP5, presumably through mTOR signaling.

It is widely recognized that NPY and SP binds to their respective receptors to activate their downstream signaling pathway. In the mammalian, there are five receptors for NPY, (NPY1R, 2R, 3R, 4R and 5R); while there is only one receptor for SP - NK1R. These G-protein-coupled receptors, when activated, could trigger multiple signaling pathways, including MEK/EKR; PI3K/AKT/mTOR. EKR1/2 is a central signaling pathway that regulates numerous cellular processes, including proliferation, differentiation and cell survival, and participated in the branching morphogenesis of epithelial organs [160]. Our data presented that both NPY and SP can induce the ERK1/2 activation at both pseudoglandular and canalicular stages of salivary gland development. (Figure 7A) Consistent with other literatures, pharmacological inhibition of the MEK, upstream cascade of ERK1/2, inhibited the epithelial branching of embryonic salivary gland (Figure 7B-7C) [160]. Additionally, we also observed a reduction in the innervated neuron after treatment of ERK1/2 inhibitor, suggested that the neuropeptide-induced neurogenesis is blocked. These results are consistent with several earlier reports illustrated that NPY

and/or SP can stimulate neuron proliferation/differentiation through ERK1/2 activation. Out data proposed that ERK1/2 is an important downstream signaling for NPY/SP-induced branching morphogenesis.

We hypothesized that the NPY and SP activated their respective receptors to promoted the branching morphogenesis. However, the qRT-PCR results showed no significant change in the expression of these receptors between control and treated samples (Supplementary Figure 1), therefore we conducted a high throughput RNA-seq analysis to identify the potential targets that got altered by neuropeptide treatment. RNA-seqs results demonstrated neuropeptide treatment altered the gene expression in biological processes related with salivary gland organogenesis such as nervous system development, cell cycles, *in utero* embryonic development, and fibroblast growth factor receptor signaling pathway. Fibroblast growth factors signaling is one cornerstone of the salivary gland development. FGF1/2/3/7/8/10/13 are expressed in the mesenchyme, while FGF1/8/10 are expressed in the epithelium [48,161]. All four type of fibroblast growth factor receptors can be found in the mesenchyme, while the epithelial cells only express FGFR1 and FGFR2 [62]. FGF/FGFR signaling regulates essential biological functions such as cell survival, proliferation, migration, differentiation, embryonic development, organogenesis, tissue repair/regeneration, and metabolism [162]. Mice lacking either FGFR1 or FGFR2 exhibits salivary gland hypoplasia, with severe effects observed in FGFR2 KO mice than FGFR1 KO mice [62]. FGF receptors are composed by an extracellular ligand consist of three immunoglobulin-like domains, a single transmembrane domain and an intracellular domain that exhibits tyrosine kinase activity [162]. Our data showed that several genes in the FGF signaling are upregulated after treatment of neuropeptide to embryonic salivary gland. Pharmacologically blocking of FGF/FGFR signal by pan-inhibitor BGJ398 abrogated the neuropeptide-induced FGFs upregulation, branching morphogenesis, and acinar differentiation, as demonstrated in Figure 9-Figure 10. Upon receptors activation, FGF receptors canonically stimulate multiple signal transduction cascades, including ERK1/2,

PI3K, and p38. Western blot data verified the activation of FGF/FGFR pathway, upregulation of acinar secretory markers Aqp5 and ductal lumen markers ZO-1 after NPY/SP treatment. The neuropeptide-induced effects are diminished during co-treatment of BGJ398 (Figure 10C). Additionally, genetic silencing of either FGFR1 or FGFR2 reverted the neuropeptide-induced branching morphogenesis to the control baseline, thus providing evidences for the involvement of FGF/FGFR signaling pathway after treatment of neuropeptides NPY or SP in embryonic salivary glands (Figure 11). It also proposed that an intact FGF/FGFR receptors signaling is necessary for beneficial effects induced by neuropeptide NPY/SP.

The connection between neuropeptides NPY and SP and the fibroblast growth factors were recorded in previous literatures. Additionally, neuropeptide treatment and FGF/FGFR signaling demonstrated synergistic effects on inducing neural cell proliferation *in vitro.* NPY administration increases FGFR1 transcription and translation, and SP administration induces the expression of FGF7 in fibroblasts of the cornea. Conversely, FGF2 induces the expression of SP and its receptor TAC1R in articular chondrocytes during the inflammatory response [164-166]. These findings are similar to our results. These results suggest that the neuropeptides NPY/SP promote development in the embryonic salivary gland, partially through interaction with the FGF/FGFR signaling pathway. However, FGFs or FGFRs that directly promote aging-induced salivary gland dysfunction and neurogenesis have not been identified.

VI. CONCLUSION

In this study, embryonic salivary gland branching morphogenesis of $kl^{+/+}$ and $kl^{-/-}$ was examined, and effects of neuropeptide treatment on embryonic salivary glands were investigated using numerous methods, and these conclusion was obtained:

In the aging mouse model (Klotho -/-), branching morphogenesis, neurogenesis, and differentiation are decreased in the embryonic salivary gland. We examined the potential effects and mechanisms of two neuropeptides, NPY and SP, on embryonic salivary gland development in aging Kl-/- mice. These results showed that administration of NPY or SP significantly promoted branching morphogenesis, neurogenesis, epithelial proliferation and epithelial differentiation through the FGF/FGFR/ERK1/2 signaling pathway during embryonic salivary gland development. Understanding the molecular signaling involved in embryonic salivary gland development during aging can greatly increase our understanding of salivary gland biology and aid in diagnosing the disease state during aging and help to identify potential therapeutic targets for regeneration and tissue engineering approaches in the future.

REFERENCES

1. Chibly AM, Aure MH, Patel VN, Hoffman MP. Salivary gland function, development, and regeneration. *Physiol Rev.* 2022;102(3):1495-1552.

2. Pedersen A, Sørensen CE, Proctor GB, Carpenter GH. Salivary functions in mastication, taste and textural perception, swallowing and initial digestion. *Oral Dis.* 2018;24(8):1399-1416. doi:10.1111/odi.12867

3. Rocchi C, Emmerson E. Mouth-Watering Results: Clinical Need, Current Approaches, and Future Directions for Salivary Gland Regeneration. *Trends Mol Med.* 2020;26(7):649-669. 10.1016/j.molmed.2020.03.009

4. Xu F, Laguna L, Sarkar A. Aging-related changes in quantity and quality of saliva: Where do we stand in our understanding?. *J Texture Stud.* 2019;50(1):27-35.

5. Li N, Ye Y, Wu Y, et al. Alterations in histology of the aging salivary gland and correlation with the glandular inflammatory microenvironment. *iScience.* 2023;26(5):106571.

6. Kuro-o M, Matsumura Y, Aizawa H, et al. Mutation of the mouse klotho gene leads to a syndrome resembling ageing. *Nature.* 1997;390(6655):45-51.

7. Amano I, Imaizumi Y, Kaji C, Kojima H, Sawa Y. Expression of podoplanin and classical cadherins in salivary gland epithelial cells of klotho-deficient mice. *Acta Histochem Cytochem.* 2011;44(6):267-276.

8. Kwon SM, Kim SA, Yoon JH, Yook JI, Ahn SG. Global analysis of gene expression profiles in the submandibular salivary gland of klotho knockout mice. *J Cell Physiol.* 2018;233(4):3282-3294.

9. Tai, N. C., Kim, S. A., & Ahn, S. G. (2019). Soluble klotho regulates the function of salivary glands by activating KLF4 pathways. *Aging (Albany NY)*, 2019;11 (19), 8254 - 8269.

10. Toan NK, Tai NC, Kim SA, Ahn SG. Choline Acetyltransferase Induces the Functional Regeneration of the Salivary Gland in Aging SAMP1/Kl -/- Mice. *Int J Mol Sci.* 2021;22(1):404.

11. Toan NK, Kim SA, Ahn SG. Ascorbic acid induces salivary gland function

through TET2/acetylcholine receptor signaling in aging SAMP1/Klotho (-/-) mice. *Aging (Albany NY)*. 2022;14(15):6028-6046.

12. Russo AF. Overview of Neuropeptides: Awakening the Senses?. *Headache*. 2017;57 Suppl 2(Suppl 2):37-46.

13. Bauer FE, Ghatei MA, Zintel A, Bloom SR. Galanin: hydrokinetic action on salivary glands in man. *Aliment Pharmacol Ther*. 1989;3(6):591-596.

14. Nedvetsky PI, Emmerson E, Finley JK, et al. Parasympathetic innervation regulates tubulogenesis in the developing salivary gland. *Dev Cell*. 2014;30(4):449-462.

15. Lee K, Kim YJ, Choi LM, et al. Human salivary gland cells express bradykinin receptors that modulate the expression of proinflammatory cytokines. *Eur J Oral Sci*. 2017;125(1):18-27.

16. Sato T, Yajima T, Fujita M, et al. Orexin A and B in the rat superior salivatory nucleus. *Auton Neurosci*. 2020;228:102712.

17. Melo IS, Candeia-Medeiros N, Ferro JNS, et al. Restoration of Cyclo-Gly-Pro-induced salivary hyposecretion and submandibular composition by naloxone in mice. *PLoS One*. 2020;15(3):e0229761.

18. Ekström J, Ekman R, Luts A, Sundler F, Tobin G. Neuropeptide Y in salivary glands of the rat: origin, release and secretory effects. *Regul Pept*. 1996;61(2):125-134.

19. Yu JH, Burns SM, Schneyer CA. Salivary secretion induced by substance P. *Proc Soc Exp Biol Med*. 1983;173(4):467-470.

20. Zhang Y, Liu CY, Chen WC, et al. Regulation of neuropeptide Y in body microenvironments and its potential application in therapies: a review. *Cell Biosci*. 2021;11(1):151.

21. Michalkiewicz M, Knestaut KM, Bytchkova EY, Michalkiewicz T. Hypotension and reduced catecholamines in neuropeptide Y transgenic rats. *Hypertension*. 2003;41(5):1056-1062.

22. Marco B, Alessandro R, Philippe F, Fabio B, Paolo R, Giulio F. The Effect of Aging on Nerve Morphology and Substance P Expression in Mouse and

Human Corneas. *Invest Ophthalmol Vis Sci.* 2018;59(13):5329-5335.

23. Redkiewicz P. The Regenerative Potential of Substance P. *Int J Mol Sci.* 2022;23(2):750.

24. Patel VN, Hoffman MP. Salivary gland development: a template for regeneration. *Semin Cell Dev Biol.* 2014;25-26:52-60.

25. Dawes C, Pedersen AM, Villa A, et al. The functions of human saliva: A review sponsored by the World Workshop on Oral Medicine VI. *Arch Oral Biol.* 2015;60(6):863-874.

26. Vila T, Rizk AM, Sultan AS, Jabra-Rizk MA. The power of saliva: Antimicrobial and beyond. *PLoS Pathog.* 2019;15(11):e1008058.

27. Frenkel ES, Ribbeck K. Salivary mucins in host defense and disease prevention. *J Oral Microbiol.* 2015;7:29759.

28. Brand HS, Ligtenberg AJ, Veerman EC. Saliva and wound healing. *Monogr Oral Sci.* 2014;24:52-60.

29. Proctor GB, Carpenter GH. Regulation of salivary gland function by autonomic nerves. *Auton Neurosci.* 2007;133(1):3-18.

30. Kondo Y, Nakamoto T, Jaramillo Y, Choi S, Catalan MA, Melvin JE. Functional differences in the acinar cells of the murine major salivary glands. *J Dent Res.* 2015;94(5):715-721.

31. Proctor GB. The physiology of salivary secretion. *Periodontol 2000.* 2016;70(1):11-25.

32. Ferreira JN, Hoffman MP. Interactions between developing nerves and salivary glands. *Organogenesis.* 2013;9(3):199-205.

33. Verstappen GM, Pringle S, Bootsma H, Kroese FGM. Epithelial-immune cell interplay in primary Sjögren syndrome salivary gland pathogenesis. *Nat Rev Rheumatol.* 2021;17(6):333-348.

34. Redman RS. Myoepithelium of salivary glands. *Microsc Res Tech.* 1994;27(1):25-45.

35. Kwon HR, Nelson DA, DeSantis KA, Morrissey JM, Larsen M. Endothelial cell regulation of salivary gland epithelial patterning. *Development.*

2017;144(2):211-220.

36. Ambudkar I. Calcium signaling defects underlying salivary gland dysfunction. *Biochim Biophys Acta Mol Cell Res.* 2018;1865(11 Pt B):1771-1777.

37. Bragiel AM, Wang D, Pieczonka TD, Shono M, Ishikawa Y. Mechanisms Underlying Activation of α_1 -Adrenergic Receptor-Induced Trafficking of AQP5 in Rat Parotid Acinar Cells under Isotonic or Hypotonic Conditions. *Int J Mol Sci.* 2016;17(7):1022.

38. Catalán MA, Kondo Y, Peña-Munzenmayer G, et al. A fluid secretion pathway unmasked by acinar-specific Tmem16A gene ablation in the adult mouse salivary gland. *Proc Natl Acad Sci U S A.* 2015;112(7):2263-2268.

39. Mukaibo T, Munemasa T, George AT, et al. The apical anion exchanger Slc26a6 promotes oxalate secretion by murine submandibular gland acinar cells. *J Biol Chem.* 2018;293(17):6259-6268.

40. Zinn VZ, Khatri A, Mednieks MI, Hand AR. Localization of cystic fibrosis transmembrane conductance regulator signaling complexes in human salivary gland striated duct cells. *Eur J Oral Sci.* 2015;123(3):140-148.

41. Gautam D, Heard TS, Cui Y, Miller G, Bloodworth L, Wess J. Cholinergic stimulation of salivary secretion studied with M1 and M3 muscarinic receptor single- and double-knockout mice. *Mol Pharmacol.* 2004;66(2):260-267.

42. Nakamura T, Matsui M, Uchida K, et al. M(3) muscarinic acetylcholine receptor plays a critical role in parasympathetic control of salivation in mice. *J Physiol.* 2004;558(Pt 2):561-575.

43. Tovey SC, Taylor CW. Cyclic AMP directs inositol (1,4,5)-trisphosphate-evoked Ca2+ signalling to different intracellular Ca2+ stores. *J Cell Sci.* 2013;126(Pt 10):2305-2313.

44. Hein P, Michel MC. Signal transduction and regulation: are all alpha1-adrenergic receptor subtypes created equal?. *Biochem Pharmacol.* 2007;73(8):1097-1106.

45. Kondo Y, Melvin JE, Catalan MA. Physiological cAMP-elevating secretagogues differentially regulate fluid and protein secretions in mouse

submandibular and sublingual glands. *Am J Physiol Cell Physiol.* 2019;316(5):C690-C697.

46. Imbery JF, Bhattacharya S, Khuder S, et al. cAMP-dependent recruitment of acidic organelles for Ca2+ signaling in the salivary gland. *Am J Physiol Cell Physiol.* 2016;311(5):C697-C709.

47. Del Fiacco M, Quartu M, Ekström J, et al. Effect of the neuropeptides vasoactive intestinal peptide, peptide histidine methionine and substance P on human major salivary gland secretion. *Oral Dis.* 2015;21(2):216-223.

48. Suzuki A, Ogata K, Iwata J. Cell signaling regulation in salivary gland development. *Cell Mol Life Sci.* 2021;78(7):3299-3315.

49. Tucker AS. Salivary gland development. *Semin Cell Dev Biol.* 2007;18(2):237-244.

50. Goodwin K, Nelson CM. Branching morphogenesis. *Development.* 2020;147(10):dev184499.

51. Myllymäki SM, Mikkola ML. Inductive signals in branching morphogenesis - lessons from mammary and salivary glands. *Curr Opin Cell Biol.* 2019;61:72-78.

52. Knosp WM, Knox SM, Lombaert IM, Haddox CL, Patel VN, Hoffman MP. Submandibular parasympathetic gangliogenesis requires sprouty-dependent Wnt signals from epithelial progenitors. *Dev Cell.* 2015;32(6):667-677.

53. Knox SM, Lombaert IMA, Reed X, Vitale-Cross L, Gutkind JS, Hoffman MP. Parasympathetic innervation maintains epithelial progenitor cells during salivary organogenesis. *Science.* 2010;329:1645 - 1647.

54. Wang S, Sekiguchi R, Daley WP, Yamada KM. Patterned cell and matrix dynamics in branching morphogenesis. *J Cell Biol.* 2017;216(3):559-570.

55. Hauser BR, Aure MH, Kelly MC; Genomics and Computational Biology Core, Hoffman MP, Chibly AM. Generation of a Single-Cell RNAseq Atlas of Murine Salivary Gland Development. *iScience.* 2020;23(12):101838.

56. Sekiguchi R, Martin D; Genomics and Computational Biology Core, Yamada KM. Single-Cell RNA-seq Identifies Cell Diversity in Embryonic Salivary

Glands. *J Dent Res*. 2020;99(1):69-78.

57. Emmerson E, Knox SM. Salivary gland stem cells: A review of development, regeneration and cancer. *Genesis*. 2018;56(5):e23211.

58. De Moerlooze L, Spencer-Dene B, Revest JM, Hajihosseini M, Rosewell I, Dickson C. An important role for the IIIb isoform of fibroblast growth factor receptor 2 (FGFR2) in mesenchymal-epithelial signalling during mouse organogenesis. *Development*. 2000;127(3):483-492.

59. Ohuchi H, Hori Y, Yamasaki M, et al. FGF10 acts as a major ligand for FGF receptor 2 IIIb in mouse multi-organ development. *Biochem Biophys Res Commun*. 2000;277(3):643-649.

60. May AJ, Chatzeli L, Proctor GB, Tucker AS. Salivary Gland Dysplasia in Fgf10 Heterozygous Mice: A New Mouse Model of Xerostomia. *Curr Mol Med*. 2015;15(7):674-682.

61. Jaskoll T, Abichaker G, Witcher D, et al. FGF10/FGFR2b signaling plays essential roles during in vivo embryonic submandibular salivary gland morphogenesis. *BMC Dev Biol*. 2005;5:11.

62. Ray AT, Soriano P. FGF signaling regulates salivary gland branching morphogenesis by modulating cell adhesion. *Development*. 2023;150(6):dev201293.

63. Steinberg Z, Myers C, Heim VM, et al. FGFR2b signaling regulates ex vivo submandibular gland epithelial cell proliferation and branching morphogenesis. *Development*. 2005;132(6):1223-1234.

64. Lombaert IM, Abrams SR, Li L, et al. Combined KIT and FGFR2b signaling regulates epithelial progenitor expansion during organogenesis. *Stem Cell Reports*. 2013;1(6):604-619.

65. Kashimata M, Gresik EW. Epidermal growth factor system is a physiological regulator of development of the mouse fetal submandibular gland and regulates expression of the alpha6-integrin subunit. *Dev Dyn*. 1997;208(2):149-161.

66. Häärä O, Koivisto T, Miettinen PJ. EGF-receptor regulates salivary gland branching morphogenesis by supporting proliferation and maturation of epithelial

cells and survival of mesenchymal cells. *Differentiation*. 2009;77(3):298-306.

67. May AJ, Mattingly AJ, Gaylord EA, et al. Neuronal-epithelial cross-talk drives acinar specification via NRG1-ERBB3-mTORC2 signaling. *Dev Cell*. 2022;57(22):2550-2565.e5.

68. Koyama N, Kashimata M, Sakashita H, Sakagami H, Gresik EW. EGF-stimulated signaling by means of PI3K, PLCgamma1, and PKC isozymes regulates branching morphogenesis of the fetal mouse submandibular gland. *Dev Dyn*. 2003;227(2):216-226.

69. Takamatsu K, Tanaka J, Katada R, et al. Aging-associated stem/progenitor cell dysfunction in the salivary glands of mice. *Exp Cell Res*. 2021;409(1):112889.

70. Affoo RH, Foley N, Garrick R, Siqueira WL, Martin RE. Meta-Analysis of Salivary Flow Rates in Young and Older Adults. *J Am Geriatr Soc*. 2015;63(10):2142-2151.

71. Maciejczyk M, Zalewska A, Ładny JR. Salivary Antioxidant Barrier, Redox Status, and Oxidative Damage to Proteins and Lipids in Healthy Children, Adults, and the Elderly. *Oxid Med Cell Longev*. 2019;2019:4393460.

72. Łysik D, Niemirowicz-Laskowska K, Bucki R, Tokajuk G, Mystkowska J. Artificial Saliva: Challenges and Future Perspectives for the Treatment of Xerostomia. *Int J Mol Sci*. 2019;20(13):3199.

73. Dubal DB, Zhu L, Sanchez PE, et al. Life extension factor klotho prevents mortality and enhances cognition in hAPP transgenic mice. *J Neurosci*. 2015;35(6):2358-2371.

74. Hu MC, Shi M, Zhang J, et al. Klotho deficiency causes vascular calcification in chronic kidney disease. *J Am Soc Nephrol*. 2011;22(1):124-136.

75. Zeldich E, Chen CD, Boden E, et al. Klotho Is Neuroprotective in the Superoxide Dismutase ($SOD1^{G93A}$) Mouse Model of ALS. *J Mol Neurosci*. 2019;69(2):264-285.

76. Ligumsky H, Merenbakh-Lamin K, Keren-Khadmy N, Wolf I, Rubinek T. The role of α-klotho in human cancer: molecular and clinical aspects. *Oncogene*.

2022;41(40):4487-4497.

77. Kurosu H, Yamamoto M, Clark JD, et al. Suppression of aging in mice by the hormone Klotho. *Science*. 2005;309(5742):1829-1833.

78. Haussler MR, Whitfield GK, Kaneko I, et al. The role of vitamin D in the FGF23, klotho, and phosphate bone-kidney endocrine axis. *Rev Endocr Metab Disord*. 2012;13(1):57-69.

79. Kurosu H, Ogawa Y, Miyoshi M, et al. Regulation of fibroblast growth factor-23 signaling by klotho. *J Biol Chem*. 2006;281(10):6120-6123.

80. Gattineni J, Bates C, Twombley K, et al. FGF23 decreases renal NaPi-2a and NaPi-2c expression and induces hypophosphatemia in vivo predominantly via FGF receptor 1. *Am J Physiol Renal Physiol*. 2009;297(2):F282-F291.

81. Hu MC, Shi M, Zhang J, et al. Klotho: a novel phosphaturic substance acting as an autocrine enzyme in the renal proximal tubule. *FASEB J*. 2010;24(9):3438-3450.

82. Chanakul A, Zhang MY, Louw A, et al. FGF-23 regulates CYP27B1 transcription in the kidney and in extra-renal tissues. *PLoS One*. 2013;8(9):e72816.

83. Lin Y, Sun Z. Antiaging gene Klotho enhances glucose-induced insulin secretion by up-regulating plasma membrane levels of TRPV2 in MIN6 β-cells. *Endocrinology*. 2012;153(7):3029-3039.

84. Lu P, Boros S, Chang Q, Bindels RJ, Hoenderop JG. The beta-glucuronidase klotho exclusively activates the epithelial Ca2+ channels TRPV5 and TRPV6. *Nephrol Dial Transplant*. 2008;23(11):3397-3402.

85. Yamamoto M, Clark JD, Pastor JV, et al. Regulation of oxidative stress by the anti-aging hormone klotho. *J Biol Chem*. 2005;280(45):38029-38034.

86. Miao J, Huang J, Luo C, et al. Klotho retards renal fibrosis through targeting mitochondrial dysfunction and cellular senescence in renal tubular cells. *Physiol Rep*. 2021;9(2):e14696.

87. Sahu A, Mamiya H, Shinde SN, et al. Age-related declines in α-Klotho drive progenitor cell mitochondrial dysfunction and impaired muscle regeneration.

Nat Commun. 2018;9(1):4859.

88. Lim SW, Jin L, Luo K, et al. Klotho enhances FoxO3-mediated manganese superoxide dismutase expression by negatively regulating PI3K/AKT pathway during tacrolimus-induced oxidative stress. *Cell Death Dis.* 2017;8(8):e2972.

89. Cui W, Leng B, Wang G. Klotho protein inhibits H2O2-induced oxidative injury in endothelial cells via regulation of PI3K/AKT/Nrf2/HO-1 pathways. *Can J Physiol Pharmacol.* 2019;97(5):370-376.

90. Lim SW, Shin YJ, Luo K, et al. Effect of Klotho on autophagy clearance in tacrolimus-induced renal injury. *FASEB J.* 2019;33(2):2694-2706.

91. DeLaney K, Buchberger AR, Atkinson L, Gründer S, Mousley A, Li L. New techniques, applications and perspectives in neuropeptide research. *J Exp Biol.* 2018;221(Pt 3):jeb151167.

92. Hook V, Funkelstein L, Lu D, Bark S, Wegrzyn J, Hwang SR. Proteases for processing proneuropeptides into peptide neurotransmitters and hormones. *Annu Rev Pharmacol Toxicol.* 2008;48:393-423.

93. Haririan H, Andrukhov O, Böttcher M, et al. Salivary neuropeptides, stress, and periodontitis. *J Periodontol.* 2018;89(1):9-18.

94. Jasim H, Carlsson A, Hedenberg-Magnusson B, Ghafouri B, Ernberg M. Saliva as a medium to detect and measure biomarkers related to pain. *Sci Rep.* 2018;8(1):3220.

95. Tsukagoshi E, Kawaguchi M, Shinomiya T, et al. Diazepam Enhances Production of Diazepam-Binding Inhibitor (DBI), a Negative Saliva Secretion Regulator, Localized in Rat Salivary Gland. *J Pharmacol Sci.* 2011;115(2):221-229.

96. Marutsuka K, Hatakeyama K, Sato Y, Yamashita A, Sumiyoshi A, Asada Y. Immunohistological localization and possible functions of adrenomedullin. *Hypertens Res.* 2003;26 Suppl:S33-S40.

97. Gröschl M, Wendler O, Topf HG, Bohlender J, Köhler H. Significance of salivary adrenomedullin in the maintenance of oral health: stimulation of oral cell proliferation and antibacterial properties. *Regul Pept.* 2009;154(1-3):16-22.

98. Pierre JF, Heneghan AF, Wang X, Roenneburg DA, Groblewski GE, Kudsk KA. Bombesin improves adaptive immunity of the salivary gland during parenteral nutrition. *JPEN J Parenter Enteral Nutr.* 2015;39(2):190-199.

99. Endoh T, Shibukawa Y, Tsumura M, Ichikawa H, Tazaki M, Inoue T. Calcitonin gene-related peptide- and adrenomedullin-induced facilitation of calcium current in submandibular ganglion. *Arch Oral Biol.* 2011;56(2):187-193.

100. Soinila J, Soinila S. Interaction of calcitonin gene-related peptide (CGRP), substance P (SP) and conventional autonomic agonists in rat submandibular salivary peroxidase release in vitro. *Auton Neurosci.* 2001;86(3):163-169.

101. Mori M, Takeuchi H, Sato M, Sumitomo S. Antimicrobial peptides in saliva and salivary glands: Their roles in the oral defense system. *Oral Med Pathol.* 2006;11(1):1 - 17.

102. Akaddar A, Doderer-Lang C, Marzahn MR, et al. Catestatin, an endogenous chromogranin A-derived peptide, inhibits in vitro growth of Plasmodium falciparum. *Cell Mol Life Sci.* 2010;67(6):1005-1015.

103. Makita T, Sucov HM, Gariepy CE, Yanagisawa M, Ginty DD. Endothelins are vascular-derived axonal guidance cues for developing sympathetic neurons. *Nature*. 2008;452(7188):759-763.

104. Ventimiglia MS, Rodriguez MR, Morales VP, et al. Endothelins participate in the central and peripheral regulation of submandibular gland secretion in the rat. *Am J Physiol Regul Integr Comp Physiol.* 2011;300(1):R109-R120.

105. Mori, M., Namba, M., Muramatsu, Y., Sumitomo, S., Takai, Y., and Shikimori,M. Endothelin expression in salivary gland. *Int. J. Oral Sci.* 2011;8(1):7 - 10.

106. Aras HC, Ekström J. Cholecystokinin- and gastrin-induced protein and amylase secretion from the parotid gland of the anaesthetized rat. *Regul Pept.* 2006;134(2-3):89-96.

107. Matoba Y, Nonaka N, Takagi Y, et al. Pituitary adenylate cyclase-activating polypeptide enhances saliva secretion via direct binding to PACAP receptors of major salivary glands in mice. *Anat Rec (Hoboken).*

2016;299(9):1293-1299.

108. Lamy E, Neves S, Ferreira J, et al. Effects of hyperleptinemia in rat saliva composition, histology and ultrastructure of the major salivary glands. *Arch Oral Biol.* 2018;96:1-12.

109. Ahmed A, Gulino A, Amayo S, et al. Natriuretic peptide system expression in murine and human submandibular salivary glands: a study of the spatial localisation of ANB, BNP, CNP and their receptors. *J Mol Histol.* 2020;51(1):3-13.

110. Turner JT, Yu H. Identification of functional receptors for vasoactive intestinal peptide and neurotensin in the human submandibular gland duct cell line, HSG-PA. *Regul Pept.* 1991;36(2):173-182.

111. Zolotukhin S. Metabolic hormones in saliva: origins and functions. *Oral Dis.* 2013;19(3):219-229.

112. Filková M, Haluzík M, Gay S, Senolt L. The role of resistin as a regulator of inflammation: Implications for various human pathologies. *Clin Immunol.* 2009;133(2):157-170.

113. Mori, M.; Sumitomo, S.; Shrestha, P.; Tanaka, S.; Takai, Y.; Shikimori, M. Multifunctional roles of growth factors or biologically active peptides in salivary glands and saliva. *Oral Med Pathol* 2008;12(4):115 - 123.

114. Tatemoto K, Carlquist M, Mutt V. Neuropeptide Y--a novel brain peptide with structural similarities to peptide YY and pancreatic polypeptide. *Nature.* 1982;296(5858):659-660.

115. Marek KL, Mains RE. Biosynthesis, development, and regulation of neuropeptide Y in superior cervical ganglion culture. *J Neurochem.* 1989;52(6):1807-1816.

116. Shende P, Desai D. Physiological and Therapeutic Roles of Neuropeptide Y on Biological Functions. *Adv Exp Med Biol.* 2020;1237:37-47.

117. Smiałowska M, Domin H, Zieba B, et al. Neuroprotective effects of neuropeptide Y-Y2 and Y5 receptor agonists in vitro and in vivo. *Neuropeptides.* 2009;43(3):235-249.

118. Chiba T, Tamashiro Y, Park D, et al. A key role for neuropeptide Y in lifespan extension and cancer suppression via dietary restriction. *Sci Rep*. 2014;4:4517.

119. Decressac M, Pain S, Chabeauti PY, et al. Neuroprotection by neuropeptide Y in cell and animal models of Parkinson's disease. *Neurobiol Aging*. 2012;33(9):2125-2137.

120. Ferreira R, Santos T, Cortes L, et al. Neuropeptide Y inhibits interleukin-1 beta-induced microglia motility. *J Neurochem*. 2012;120(1):93-105.

121. Spencer B, Potkar R, Metcalf J, et al. Systemic Central Nervous System (CNS)-targeted Delivery of Neuropeptide Y (NPY) Reduces Neurodegeneration and Increases Neural Precursor Cell Proliferation in a Mouse Model of Alzheimer Disease. *J Biol Chem*. 2016;291(4):1905-1920.

122. Panossian A, Wikman G, Kaur P, Asea A. Adaptogens stimulate neuropeptide y and hsp72 expression and release in neuroglia cells. *Front Neurosci*. 2012;6:6.

123. Aveleira CA, Botelho M, Carmo-Silva S, et al. Neuropeptide Y stimulates autophagy in hypothalamic neurons. *Proc Natl Acad Sci U S A*. 2015;112(13):E1642-E1651.

124. V Euler US, Gaddum JH. An unidentified depressor substance in certain tissue extracts. *J Physiol*. 1931;72(1):74-87.

125. Nawa H, Hirose T, Takashima H, Inayama S, Nakanishi S. Nucleotide sequences of cloned cDNAs for two types of bovine brain substance P precursor. *Nature*. 1983;306(5938):32-36.

126. Harrison S, Geppetti P. Substance p. *Int J Biochem Cell Biol*. 2001;33(6):555-576.

127. Mashaghi A, Marmalidou A, Tehrani M, Grace PM, Pothoulakis C, Dana R. Neuropeptide substance P and the immune response. *Cell Mol Life Sci*. 2016;73(22):4249-4264.

128. Delgado AV, McManus AT, Chambers JP. Production of tumor necrosis factor-alpha, interleukin 1-beta, interleukin 2, and interleukin 6 by rat leukocyte

subpopulations after exposure to substance P. *Neuropeptides*. 2003;37(6):355-361.

129. Geindreau M, Bruchard M, Vegran F. Role of Cytokines and Chemokines in Angiogenesis in a Tumor Context. *Cancers (Basel)*. 2022;14(10):2446.

130. Yu J, Nam D, Park KS. Substance P enhances cellular migration and inhibits senescence in human dermal fibroblasts under hyperglycemic conditions. *Biochem Biophys Res Commun*. 2020;522(4):917-923.

131. Nagano T, Nakamura M, Nakata K, et al. Effects of substance P and IGF-1 in corneal epithelial barrier function and wound healing in a rat model of neurotrophic keratopathy. *Invest Ophthalmol Vis Sci*. 2003;44(9):3810-3815.

132. Felderbauer P, Bulut K, Hoeck K, Deters S, Schmidt WE, Hoffmann P. Substance P induces intestinal wound healing via fibroblasts--evidence for a TGF-beta-dependent effect. *Int J Colorectal Dis*. 2007;22(12):1475-1480.

133. Yang L, Li G, Ye J, et al. Substance P enhances endogenous neurogenesis to improve functional recovery after spinal cord injury. *Int J Biochem Cell Biol*. 2017;89:110-119.

134. Thornton E, Vink R. Treatment with a substance P receptor antagonist is neuroprotective in the intrastriatal 6-hydroxydopamine model of early Parkinson's disease. *PLoS One*. 2012;7(4):e34138.

135. Teshima THN, Tucker AS, Lourenço SV. Dual Sympathetic Input into Developing Salivary Glands. *J Dent Res*. 2019;98(10):1122-1130.

136. Lidsky PV, Yuan J, Rulison JM, Andino-Pavlovsky R. Is Aging an Inevitable Characteristic of Organic Life or an Evolutionary Adaptation?. *Biochemistry (Mosc)*. 2022;87(12):1413-1445.

137. Murga M, Bunting S, Montaña MF, et al. A mouse model of ATR-Seckel shows embryonic replicative stress and accelerated aging. *Nat Genet*. 2009;41(8):891-898.

138. Wang L, Yang L, Burns K, Kuan CY, Zheng Y. Cdc42GAP regulates c-Jun N-terminal kinase (JNK)-mediated apoptosis and cell number during mammalian perinatal growth. *Proc Natl Acad Sci U S A*.

2005;102(38):13484-13489.

139. Wang L, Yang L, Debidda M, Witte D, Zheng Y. Cdc42 GTPase-activating protein deficiency promotes genomic instability and premature aging-like phenotypes. *Proc Natl Acad Sci U S A.* 2007;104(4):1248-1253.

140. Sun LQ, Lee DW, Zhang Q, et al. Growth retardation and premature aging phenotypes in mice with disruption of the SNF2-like gene, PASG. *Genes Dev.* 2004;18(9):1035-1046.

141. Shiozaki M, Yoshimura K, Shibata M, et al. Morphological and biochemical signs of age-related neurodegenerative changes in klotho mutant mice. *Neuroscience.* 2008;152(4):924-941.

142. Chen CD, Sloane JA, Li H, et al. The antiaging protein Klotho enhances oligodendrocyte maturation and myelination of the CNS. *J Neurosci.* 2013;33(5):1927-1939.

143. Zeldich E, Chen CD, Colvin TA, et al. The neuroprotective effect of Klotho is mediated via regulation of members of the redox system. *J Biol Chem.* 2014;289(35):24700-24715.

144. Kim JM, Jo Y, Jung JW, Park K. A mechanogenetic role for the actomyosin complex in branching morphogenesis of epithelial organs. *Development.* 2021;148(6):dev190785.

145. Rao RK, Basuroy S, Rao VU, Karnaky KJ Jr, Gupta A. Tyrosine phosphorylation and dissociation of occludin-ZO-1 and E-cadherin-beta-catenin complexes from the cytoskeleton by oxidative stress. *Biochem J.* 2002;368(Pt 2):471-481.

146. Erickson JC, Clegg KE, Palmiter RD. Sensitivity to leptin and susceptibility to seizures of mice lacking neuropeptide Y. *Nature.* 1996;381(6581):415-421.

147. Baldock PA, Lee NJ, Driessler F, et al. Neuropeptide Y knockout mice reveal a central role of NPY in the coordination of bone mass to body weight. *PLoS One.* 2009;4(12):e8415.

148. Zimmer A, Zimmer AM, Baffi J, et al. Hypoalgesia in mice with a targeted deletion of the tachykinin 1 gene. *Proc Natl Acad Sci U S A*. **1998**;95(5):2630-2635.

149. Niedermair T, Kuhn V, Doranehgard F, et al. Absence of substance P and the sympathetic nervous system impact on bone structure and chondrocyte differentiation in an adult model of endochondral ossification. *Matrix Biol*. **2014**;38:22-35.

150. Choi Y, Tee JB, Gallegos TF, et al. Neuropeptide Y functions as a facilitator of GDNF-induced budding of the Wolffian duct. *Development*. **2009**;136(24):4213-4224.

151. Park SW, Yan YP, Satriotomo I, Vemuganti R, Dempsey RJ. Substance P is a promoter of adult neural progenitor cell proliferation under normal and ischemic conditions. *J Neurosurg*. **2007**;107(3):593-599.

152. Decressac M, Wright B, David B, et al. Exogenous neuropeptide Y promotes in vivo hippocampal neurogenesis. *Hippocampus*. **2011**;21(3):233-238.

153. Emmerson E, May AJ, Nathan S, et al. SOX2 regulates acinar cell development in the salivary gland. *Elife*. **2017**;6:e26620.

154. Emmerson E, May AJ, Berthoin L, et al. Salivary glands regenerate after radiation injury through SOX2-mediated secretory cell replacement. *EMBO Mol Med*. **2018**;10(3):e8051.

155. Lahtivirta S, Koistinaho J, Hervonen A. Effect of sialectomy on the superior cervical ganglion sympathetic neurons in young adult and aged mice. *Mech Ageing Dev*. **1992**;62(1):25-33.

156. Zhang SE, Su YX, Zheng GS, Liang YJ, Liao GQ. Reinnervated nerves contribute to the secretion function and regeneration of denervated submandibular glands in rabbits. *Eur J Oral Sci*. **2014**;122(6):372-381.

157. Li J, Sudiwala S, Berthoin L, et al. Long-term functional regeneration of radiation-damaged salivary glands through delivery of a neurogenic hydrogel. *Sci Adv*. **2022**;8(51):eadc8753.

158. Lombaert IMA, Hoffman MP. Epithelial stem/progenitor cells in the

embryonic mouse submandibular gland. *Front Oral Biol*. 2010;14:90-106.

159. Sakai M, Fukumoto M, Ikai K, et al. Role of the mTOR signalling pathway in salivary gland development. *FEBS J*. 2019;286(18):3701-3717.

160. Kashimata M, Sayeed S, Ka A, et al. The ERK-1/2 signaling pathway is involved in the stimulation of branching morphogenesis of fetal mouse submandibular glands by EGF. *Dev Biol*. 2000;220(2):183-196.

161. Hoffman MP, Kidder BL, Steinberg ZL, et al. Gene expression profiles of mouse submandibular gland development: FGFR1 regulates branching morphogenesis in vitro through BMP- and FGF-dependent mechanisms. *Development*. 2002;129(24):5767-5778.

162. Ornitz DM, Itoh N. The Fibroblast Growth Factor signaling pathway. *Wiley Interdiscip Rev Dev Biol*. 2015;4(3):215-266.

163. Rodrigo C, Zaben M, Lawrence T, Laskowski A, Howell OW, Gray WP. NPY augments the proliferative effect of FGF2 and increases the expression of FGFR1 on nestin positive postnatal hippocampal precursor cells, via the Y1 receptor. *J Neurochem*. 2010;113(3):615-627.

164. Im HJ, Li X, Muddasani P, et al. Basic fibroblast growth factor accelerates matrix degradation via a neuro-endocrine pathway in human adult articular chondrocytes. *J Cell Physiol*. 2008;215(2):452-463.

165. Foldenauer ME, McClellan SA, Barrett RP, Zhang Y, Hazlett LD. Substance P affects growth factors in Pseudomonas aeruginosa-infected mouse cornea. *Cornea*. 2012;31(10):1176-1188.

166. Sideri A, Bakirtzi K, Shih DQ, et al. Substance P mediates pro-inflammatory cytokine release form mesenteric adipocytes in Inflammatory Bowel Disease patients. *Cell Mol Gastroenterol Hepatol*. 2015;1(4):420-432.